The Astrophysical Journal, 937:64 (17pp), 2022 October 1 https://doi.org/10.3847/1538-4357/ac8d5e

The Galactic Nova Rate: Estimates from the ASAS-SN and Gaia Surveys

A. Kawash[1], L. Chomiuk[1], J. Strader[1], K. V. Sokolovsky[1,2], E. Aydi[1], C. S. Kochanek[3,4], K. Z. Stanek[3,4], Z. Kostrzewa-Rutkowska[5,6], S. T. Hodgkin[7], K. Mukai[8,9], B. Shappee[10], T. Jayasinghe[3], M. Rizzo Smith[3], T. W.-S. Holoien[11], J. L. Prieto[12,13], and T. A. Thompson[3,4]

[1] Center for Data Intensive and Time Domain Astronomy, Department of Physics and Astronomy, Michigan State University, East Lansing, MI 48824, USA
kawashad@msu.edu
[2] Sternberg Astronomical Institute, Moscow State University, Universitetskii pr. 13, 119992 Moscow, Russia
[3] Department of Astronomy, The Ohio State University, 140 West 18th Avenue, Columbus, OH 43210, USA
[4] Center for Cosmology and Astroparticle Physics, The Ohio State University, 191 W. Woodruff Avenue, Columbus, OH 43210, USA
[5] Leiden Observatory, Leiden University, PO Box 9513, 2300 RA Leiden, The Netherlands
[6] SRON Netherlands Institute for Space Research, Niels Bohrweg 4, 2333 CA Leiden, The Netherlands
[7] Institute of Astronomy, Madingley Road, Cambridge CB3 0HA, UK
[8] CRESST II and X-ray Astrophysics Laboratory, NASA/GSFC, Greenbelt, MD 20771, USA
[9] Department of Physics, University of Maryland, Baltimore County, 1000 Hilltop Circle, Baltimore, MD 21250, USA
[10] Institute for Astronomy, University of Hawaiì at Mānoa, 2680 Woodlawn Dr., Honolulu, HI 96822, USA
[11] Carnegie Observatories, 813 Santa Barbara Street, Pasadena, CA 91101, USA
[12] Núcleo de Astronomía de la Facultad de Ingeniería y Ciencias, Universidad Diego Portales, Av. Ejército 441, Santiago, Chile
[13] Millennium Institute of Astrophysics, Santiago, Chile
Received 2022 June 27; revised 2022 August 12; accepted 2022 August 26; published 2022 September 29

Abstract

We present the first estimate of the Galactic nova rate based on optical transient surveys covering the entire sky. Using data from the All-Sky Automated Survey for Supernovae (ASAS-SN) and Gaia—the only two all-sky surveys to report classical nova candidates—we find 39 confirmed Galactic novae and 7 additional unconfirmed candidates discovered from 2019 to 2021, yielding a nova discovery rate of $\approx 14\,\mathrm{yr}^{-1}$. Using accurate Galactic stellar mass models and three-dimensional dust maps and incorporating realistic nova light curves, we have built a sophisticated Galactic nova model to estimate the fraction of Galactic novae discovered by these surveys over this time period. The observing capabilities of each survey are distinct: the high cadence of ASAS-SN makes it sensitive to fast novae, while the broad observing filter and high spatial resolution of Gaia make it more sensitive to highly reddened novae across the entire Galactic plane and bulge. Despite these differences, we find that ASAS-SN and Gaia give consistent Galactic nova rates, with a final joint nova rate of $26 \pm 5\,\mathrm{yr}^{-1}$. This inferred nova rate is substantially lower than found by many other recent studies. Critically assessing the systematic uncertainties in the Galactic nova rate, we argue that the role of faint, fast-fading novae has likely been overestimated, but that subtle details in the operation of transient alert pipelines can have large, sometimes unappreciated effects on transient recovery efficiency. Our predicted nova rate can be directly tested with forthcoming red/near-infrared transient surveys in the southern hemisphere.

Unified Astronomy Thesaurus concepts: Classical novae (251); Novae (1127); Cataclysmic variable stars (203); White dwarf stars (1799)

1. Introduction

A classical nova eruption is the result of a thermonuclear runaway of accreted hydrogen-rich material on the surface of a white dwarf (see Warner 2008; Chomiuk et al. 2021 for reviews). At peak brightness, novae are relatively luminous, with absolute magnitudes between $M_V \approx -4$ and -10 mag (Shafter 2017), allowing them to be discovered out to the largest Galactic distances and in nearby galaxies. Discoveries of Galactic novae date back thousands of years (Patterson et al. 2013; Shara et al. 2017b), and estimates of the total frequency with which the Milky Way produces novae date back nearly a century (Lundmark 1935). The nova rate has broad implications in a range of areas, including Galactic nucleosynthesis, binary evolution, and the origin of Type Ia supernovae.

Found in both the Galactic disk and bulge, novae have long been thought to be significant contributors to the Galactic abundance of specific isotopes, including by-products of the CNO cycle (^{13}C, ^{15}N, and ^{17}O) and those that radioactively decay (^{7}Be, ^{22}Na, and ^{26}Al; José & Hernanz 1998). To quantify these contributions, we need not only to understand how these isotopes are created and how much of them are ejected in individual eruptions but also to have a solid estimate of the Galactic nova rate. Take, for example, ^{7}Be—the creation of which has been suggested in nova explosions for decades (Arnould & Norgaard 1975; Starrfield et al. 1978). However, predictions for the amount of ^{7}Be created in a typical nova were uncertain (José & Hernanz 1998). ^{7}Be was recently detected in the ejecta of V339 Del and V5668 Sgr, placing yields on more solid ground (Tajitsu et al. 2015; Izzo et al. 2015). ^{7}Be decays to ^{7}Li with a half-life of 53.22 days, so nova eruptions could be responsible for a significant amount of the present-day Galactic abundance of lithium (Romano et al. 2001; Prantzos 2012; Rukeya et al. 2017; Starrfield et al. 2020).

Another radioactive isotope created during a nova eruption is ^{26}Al (José & Hernanz 1998). This isotope, observed via its MeV γ-ray line emission, is also produced in supernovae and has been used as a tracer of the Galactic supernova rate and star

formation rate (Diehl et al. 2006). However, the recent study of Vasini et al. (2022) shows that novae are likely to be significant contributors to the Galactic ^{26}Al budget, perhaps accounting for the majority of the ^{26}Al mass (see also Bennett et al. 2013). The uncertainty in the nova rate makes determining such nucleosynthetic contributions difficult.

In addition to being an important input to chemical evolution models, the Galactic nova rate is also a constraint on binary population synthesis models (Chen et al. 2016; Kemp et al. 2021). It has recently been realized that nova eruptions may be an important mechanism of angular momentum loss from interacting close binary systems (Schenker et al. 1998; Schreiber et al. 2016; Pala et al. 2022) affecting their evolutionary outcome (Nelemans et al. 2016; Sparks & Sion 2021; Metzger et al. 2021). In addition, some novae could be the progenitors to Type Ia supernovae (e.g., Patat et al. 2011; Dilday et al. 2012; Darnley et al. 2015), depending on the degree to which white dwarfs can retain accreted mass over the course of a nova eruption (Toonen et al. 2014; Starrfield et al. 2020). Binary models can now reproduce the zoo of accreting white dwarf binaries (Kalomeni et al. 2016), and, in the future, a comparison of nova rates with other white dwarf binary populations can shed light on how and when white dwarfs manage to grow in mass.

Determining the nova rate of the Milky Way is also important for understanding which—and how many—novae are currently missing from our samples of discovered Galactic novae. Galactic novae are the eruptions we can study in great detail, bringing to bear observations from radio to γ-ray wavelengths and revealing the physics that drives these eruptions (Chomiuk et al. 2021). However, it is unclear whether the targets of these detailed studies are a representative sample, or whether particular kinds of novae are missing from our current Galactic samples.

For these reasons, constraining the Galactic nova rate is important, but it has proven to be a tricky problem. Below we summarize the efforts of the community in discovering Galactic classical novae and the published predictions of the frequency at which novae are produced in the Milky Way.

1.1. History of Nova Discoveries

Though discoveries of Galactic novae date back millennia, the systematic monitoring of the sky for novae by photographic means began around the turn of the twentieth century (Duerbeck 2008). During the first half of the twentieth century, $\sim$2 novae were discovered per year visually and using photographic plates. With the widespread use of astronomical photography (Pickering 1893, 1895) and the advent of objective prism surveys (Duerbeck 2008), the rate of discoveries increased to $\sim$3 yr^{-1} in the mid-twentieth century. In the 1980s and 1990s, film photography became commonly used by amateur astronomers, and the discovery rate increased to $\sim$4 yr^{-1}.

In the 2000s and 2010s, more sensitive large-format CCD and CMOS-based digital cameras became widely available to amateur astronomers, increasing the annual nova discovery rate to $\sim$8 yr^{-1} (see Figure 1). It was thought that discoveries were highly incomplete (Liller & Mayer 1987), but the degree to which novae were missed owing to a shallow magnitude limit, low observational cadence, or lack of sky coverage was unknown. Therefore, it was unclear whether professional surveys with systematic observations would produce a large increase in the discovery rate.

The All-sky Automated Survey (ASAS-3; Pojmański 2001) was one of the first CCD surveys imaging the entire sky reachable from its observing site and contributed to nova discoveries in the early 2000s. Many surveys at the time were focused on searching for supernovae, asteroids, or transiting exoplanets, so observations of transients in the Galactic plane were lacking, but surveys like ASAS-3 inspired the next generation of wide-field nova searches.

In the 2010s, large sky surveys began to contribute significantly to the discovery of Galactic novae. The Fourth Phase of the Optical Gravitational Lensing Experiment (OGLE-IV; Udalski et al. 2015) began in 2010, with high-cadence I-band observations of the central bulge discovering a large number of candidate bulge novae (Mróz et al. 2015). The New Milky Way Survey (NMW; Sokolovsky et al. 2014) began searching for transients in the northern hemisphere Galactic plane at high cadence down to $V \approx 13.5$ mag in 2011. The All-Sky Automated Survey for SuperNovae (ASAS-SN; Shappee et al. 2014) started searching for transients in 2013, and then in 2017 it became the first survey to systematically observe the entire night sky, including the Galactic plane, with nearly daily cadence down to $g \approx 18.5$ mag (Kochanek et al. 2017). These high-cadence and systematic observations allowed for fast-declining novae to be discovered anywhere on the sky. The Palomar Gattini-IR survey (PGIR; De et al. 2020f) began surveying the northern hemisphere Galactic plane in 2019 down to $J \approx 15.3$ AB mag. As a near-IR survey, PGIR can discover highly extinguished novae not discovered in previous years (De et al. 2021b). These surveys were designed to discover transients, but the astrometrically focused Gaia (Gaia Collaboration et al. 2016) has been a surprising contributor to the discovery of Galactic novae. The broad observing filter, high angular resolution, and all-sky coverage allow Gaia to detect highly reddened novae anywhere on the sky, including the southern Galactic plane (Hodgkin et al. 2021b). These surveys have helped to increase the average discovery rate to 10.5 yr^{-1} since 2010, with 17 spectroscopically confirmed novae in 2021, the highest number on record (see Figure 1). A higher discovery rate allows for better estimates of the global Galactic nova rate, as there is less sensitivity to model assumptions.

1.2. Galactic Nova Rate Predictions

Two methods have been used to estimate the total rate of classical nova production in the Galaxy. The first method extrapolates a sample of discovered Galactic novae based on the estimated completeness (commonly referred to as the Galactic or direct method). The second method estimates the rate in a nearby galaxy and infers the Milky Way rate by scaling on the relative luminosities of the two galaxies (referred to as the extragalactic or indirect method).

The direct method was used to make the first prediction for the total frequency of Galactic nova eruptions. It was estimated that there should be at least, but probably much higher than, $R = 50$ novae per year (Lundmark 1935). Two decades later, Allen (1954) used a sample of 19 novae to estimate a Galactic rate of $R \sim 100$ yr^{-1}. Kopylov (1955) used 23 novae thought to be within 1500 pc of the Sun observed over a 60 yr period, arriving at a rate of $R = 50$ Galactic novae per year. In another two decades, Sharov (1972) extrapolated from a sample of

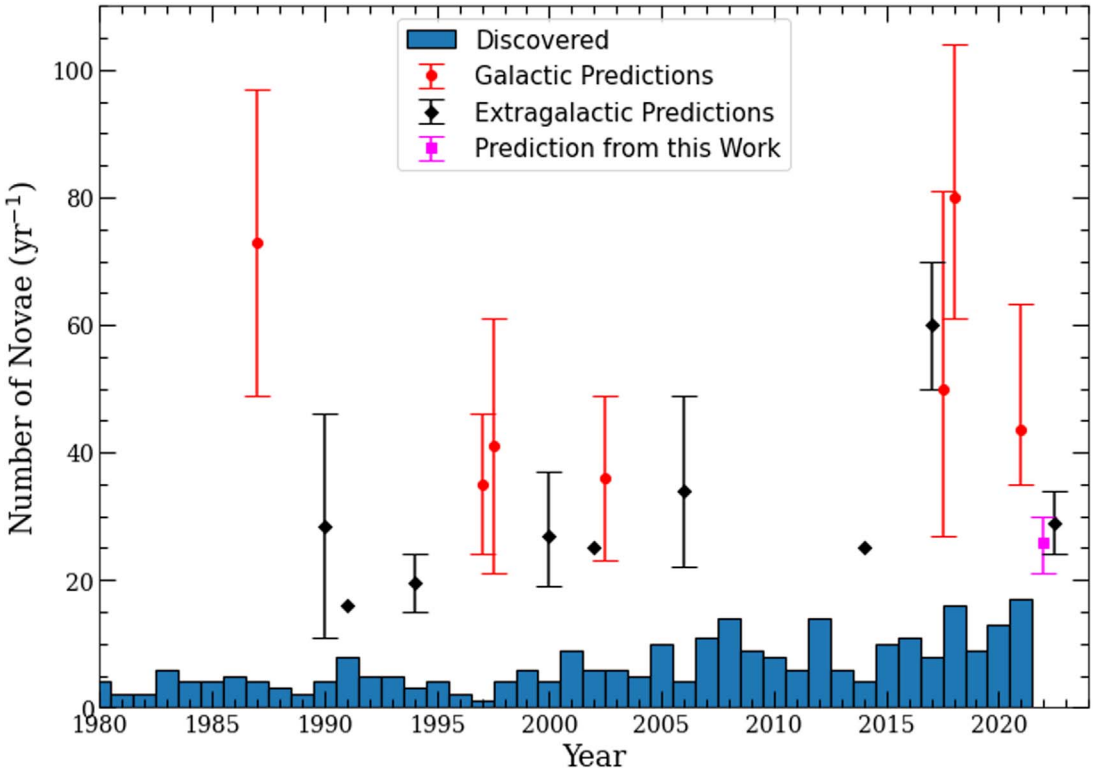

Figure 1. Galactic nova rate predictions as a function of the year published, compared with the number of novae confirmed each year since 1980. The rate predictions made using the Galactic or direct method are shown as red circles, and those using the extragalactic or indirect method are shown as black diamonds, along with error bars if the uncertainty was estimated. The estimate from this work is shown as the magenta square. The number of discovered and confirmed Galactic novae each year is plotted as a blue histogram and was derived using Koji Mukai's List of Galactic Novae, Bill Gray's Database of Galactic Novae, and AAVSO's VSX. Citations for published rates from left to right are as follows: Liller & Mayer (1987), Ciardullo et al. (1990), van den Bergh (1991b), della Valle & Livio (1994b), Shafter (1997), Hatano et al. (1997), Shafter et al. (2000), Shafter (2002), Darnley et al. (2006), Shafter et al. (2014), Shafter (2017), Özdönmez et al. (2018), De et al. (2021b), and Rector et al. (2022).

eight novae in the solar neighborhood to estimate a nova rate of $R = 259$ yr^{-1} for the entire Galaxy. In a similar fashion, Liller & Mayer (1987) extrapolated from a sample of 17 novae thought to be within a 60° slice of the Galaxy to a total rate of $R = 73 \pm 24$ yr^{-1}. Then, Hatano et al. (1997) assumed that novae in the Galaxy are disk dominated and arrived at an annual rate of $R = 41 \pm 21$ yr^{-1}.

In the 1990s, estimates began to be derived from extragalactic samples of novae using the indirect method. Ciardullo et al. (1990) used the nova rate of NGC 5128 to infer the nova rate in our own Galaxy to be between $R = 11$ and 46 yr^{-1}. Van den Bergh (1991a) considered the nova rates in M31 and M33 and the globular cluster population ratios to deduce a Galactic nova rate of $R \sim 16$ yr^{-1}. Della Valle & Livio (1994a) derived a Galactic rate of $R = 24$ yr^{-1} by measuring the rates in five other galaxies and assuming that the rates were proportional to the galaxy luminosity. Finally, Darnley et al. (2006) used a survey of M31 to infer a Galactic nova rate of $R = 34^{+15}_{-12}$ yr^{-1}. Even more recently, Rector et al. (2022) used a 20 yr survey of M31 to indirectly estimate a slightly lower Galactic nova rate of $R = 28^{+5}_{-4}$ yr^{-1}.

Shafter (1997) is the first in a series of papers that extensively looked at the Galactic nova rate and estimated, by extrapolating samples of novae of varying sector size, limiting magnitude, and time period, that the Galactic nova rate is 35 ± 11 yr^{-1}. Then, Shafter et al. (2000) estimated the nova rates in M51, M87, and M101 to indirectly estimate a Galactic nova rate of $R = 27^{+10}_{-8}$ yr^{-1}. A couple years later, Shafter (2002) assumed that the discovered sample of $m_V < 2$ mag novae is complete, extrapolated to a global rate of $R = 36 \pm 13$ yr^{-1}, and also derived a rate of $R \sim 25$ yr^{-1} by comparing the K-band luminosity and nova rate of M31 to the Milky Way. Shafter et al. (2014) indirectly estimated a Galactic nova rate of $R \sim 25$ yr^{-1} by scaling the rates of 16 galaxies by their K-band luminosities. In the most recent paper of this series, Shafter (2017) assumed that the $m_V < 2$ mag novae are 90% complete and estimated that the most likely nova rate is $R = 50^{+31}_{-23}$ yr^{-1}. An even higher rate was predicted a year later when Özdönmez et al. (2018) estimated the local density of nova eruptions to predict an average estimate of the disk nova rate of $R = 67^{+21}_{-17}$ yr^{-1}, and by combining this with a bulge rate estimate of $R = 13.8 \pm 2.6$ yr^{-1} (Mróz et al. 2015), they predicted a Galactic nova rate of $R \sim 80$ yr^{-1}.

These predictions from the past 40 years, along with the history of the nova discovery rate, are summarized in Figure 1. One noticeable feature is that the extragalactic predictions estimated lower rates on average than the recent predictions from Galactic data. The Hubble Space Telescope (HST) survey of M87 novae (Shara et al. 2016) derived a nova rate for M87 over three times larger than that estimated by Shafter et al. (2000). The authors argue that HST is more sensitive to faint and fast novae and that previous extragalactic nova surveys had underestimated nova rates because they neglected this harder-to-discover class of novae. Assuming this to be the case, the Galactic rate derived from the M31 sample in Darnley et al. (2006) was increased to between ∼50 and ∼70 yr^{-1} (Shafter 2017).

Accounting for faint and fast novae could finally make the predictions from both the direct and indirect methods consistent, but it also appears at odds with the only modest increase in the discovery rate after the advent of large sky surveys: the implication would be that we are still discovering fewer than a quarter of the Galaxy's novae. With these new surveys, it is less plausible that time sampling is the main reason that novae are being missed, so another explanation is needed. A reasonable possibility is dust—that many novae are being hidden from optical surveys by foreground extinction. Kawash et al. (2021d) quantified the contribution of interstellar dust extinction to the optical discovery rate of Galactic novae and found that dust can hide ∼50% of the Galactic population from being discovered by observers using V- or g-band filters. This helps explain some—but not all—of the discrepancy between the discovered and predicted rates.

Luckily, the well-defined observing patterns of large time-domain surveys now make it possible to make systematic predictions of the Galactic nova rate by calculating the expected completeness in the survey data. This new era of Galactic nova rate estimates from large sky surveys began with a prediction using data from PGIR, where a sample of 11 highly reddened novae was used to derive a rate of $R = 44^{+20}_{-9}$ yr^{-1} (De et al. 2021b). This is consistent with the higher rates that have been published recently, and more predictions from other large sky surveys could help bolster these higher-frequency estimates.

For the first time, in this paper we use data from multiple all-sky surveys to estimate the nova rate of the Milky Way. The use of all-sky surveys reduces the sensitivity of our results to possible differences in nova behavior between the disk and bulge (see, e.g., Della Valle & Izzo 2020).

To date, there are only two all-sky surveys that have reported a nova candidate. First, ASAS-SN became able to scan the entire night sky at a roughly 1-day cadence in 2017. This high cadence was unprecedented, allowing for the discovery of fast novae anywhere on the sky.

Gaia is the only other all-sky survey that reports nova candidates. Gaia is designed to repeatedly scan the whole sky to make astrometric measurements, and its observing pattern allows for the discovery of many transients, including novae. Usually, a pair of observations are taken 106.5 minutes apart and followed up 2–4 weeks later if the field is not Sun constrained. Though the cadence is much lower than ASAS-SN observations, the high angular resolution ($0\farcs06 \times 0\farcs18$), the broad G-band observing filter, and the limiting magnitude ($G < 19$ mag.) make Gaia sensitive to certain novae in the plane that no other survey can detect (Hodgkin et al. 2021b). Hence, these two surveys are sensitive to different types of hard-to-detect novae: ASAS-SN to fast novae and Gaia to highly reddened novae in crowded fields. Making a rate estimation using both surveys allows us to better predict the Galactic nova rate, capitalizing on both surveys' distinct strengths.

In Section 2, we discuss the sample of novae detected by the surveys and the assumptions we make to calculate the discovery rates. In Section 3, we explain how we modeled the population of Galactic novae using a Monte Carlo simulation to estimate the Galactic nova rate. Then, in Section 4 we show the results and compare the simulated detections to the real sample. In Section 5, we compare our results to previous estimates and explore how different model assumptions can change the results. Finally, in Section 6, we summarize our results and the broader implications.

2. Discovered Samples

The direct method of predicting the Galactic nova rate corrects the observed rate for survey incompleteness, typically quantified as the recovery efficiency. All spectroscopically confirmed Galactic novae discovered from 2019 to 2021 are listed in Table 1. Although both ASAS-SN and Gaia had been discovering nova candidates before 2019, the observing strategies and pipelines were less stable and hence more difficult to model. During 2019–2021, both surveys graduated to having well-understood observing strategies, and our team took on the task of spectroscopic classification of all promising nova candidates (Kawash et al. 2021a; Aydi et al. 2021; Kawash et al. 2021c, 2021b; Aydi et al. 2020b; Sokolovsky et al. 2020; Aydi et al. 2020a; Kawash et al. 2020; Aydi et al. 2019a, 2020c, 2020d; Strader et al. 2019a; Aydi et al. 2019b, 2019c, 2019d). The sample in Table 1 was arrived at by performing exhaustive searches in the ASAS-SN and Gaia databases, as discussed in the following subsections, with the goal of making it as complete as possible. Throughout this paper, we assume that any error in the discovery rate caused by nova candidates going unnoticed after being reported will be less than the Poisson errors.

In Table 1, the names and positions of the novae are taken from an online Galactic nova catalog maintained by one of us (K.M.).[14] If the nova was detected by ASAS-SN or Gaia, we list the date of first detection and the peak detected brightness for each respective survey. The peak brightness does not always occur on the date of first detection, and the peak brightness detected by a survey can be significantly fainter than the true peak brightness if a nova was first detected after a seasonal gap. V3890 Sgr and RS Oph are recurrent novae listed in Table 1. No Galactic recurrent nova erupted multiple times over this survey period, but the ASAS-SN and Gaia pipelines are capable of detecting multiple eruptions in a single system, and if such a system existed, we would have counted it as multiple eruptions when calculating the discovery rates. To be as complete as possible, we also list reported transients that were never followed up spectroscopically and could have been classical novae in Table 2 (individual objects are discussed in Sections 2.1 and 2.2).

2.1. Gaia Discovery Rate

Gaia transients are reported publicly to the Gaia science alerts (GSA) website,[15] but only 25% of GSA transients have been classified spectroscopically. The vast majority of confirmed candidates are extragalactic supernovae (Hodgkin et al. 2021b), and as seen in Figure 14 of Hodgkin et al. (2021b), there are a large number of Galactic plane transients that are not classified. Therefore, the number of confirmed classical novae reported by GSA is certainly lower than the actual number detected. To quantify this, we have searched the entire archive of GSA transients for missed Galactic nova events.

In 2021 September, we performed a retroactive nova search on the ∼17,500 transients in the GSA website. Those at high

[14] "Koji's List of Recent Galactic Novae"; https://asd.gsfc.nasa.gov/Koji.Mukai/novae/novae.html.

[15] http://gsaweb.ast.cam.ac.uk/alerts

Table 1
Confirmed Galactic Classical Novae 2019–2021

Name	RAJ2000 (h m s)	DEJ2000 (° ' ")	ASAS-SN t_0 (yyyy-mm-dd)	ASAS-SN Peak (g mag)	Gaia t_0 (yyyy-mm-dd)	Gaia Peak (G mag)	Reference
AT 2021abud	15:27:31.61	−55:06:23.8			2021-10-06	13.9	Kawash et al. (2021c)
AT 2021abxa	17:54:14.14	−24:12:23.5			2021-09-20	13.8	Kawash et al. (2021c)
AT 2021aaav	17:32:21.96	−33:01:41.5			2021-09-19	18.2	Kawash et al. (2021b)
AT 2021aadi	18:00:44.88	−21:39:40.5			2021-09-20	16.2	De et al. (2021a)
ASASSN-21pa	17:26:19.38	−33:27:10.7	2021-07-30	17.5	2021-08-22	14.9	Aydi et al. (2021)
AT 2021wkq	16:44:50.21	−45:15:48.1			2021-08-18	16.3	Kawash et al. (2021a)
RS Oph	17:50:13.17	−06:42:28.6	2021-08-10	5.8			Geary & Amorim (2021)
V0606 Vul	20:21:07.70	+29:14:09.1	2021-07-16	10.6			Munari et al. (2021a)
V1711 Sco	17:39:44.74	−36:16:40.6	2021-06-22	12.8	2021-09-18	15.5	Karambelkar et al. (2021)
V1674 Her	18:57:30.98	+16:53:39.6	2021-06-12	9.4			Munari et al. (2021b)
AT 2021nwn	19:12:38.61	+12:41:34.4			2021-05-12	15.7	De et al. (2021c)
V2030 Aql	19:07:58.62	+08:43:45.8			2021-05-13	17.3	Soria et al. (2021)
V1710 Sco	17:09:08.11	−37:30:40.9	2021-04-12	9.7			Joshi et al. (2021)
V6595 Sgr	17:58:16.09	−29:14:56.6	2021-04-05	9.0			Taguchi et al. (2021)
V6594 Sgr	18:49:05.07	−19:02:04.2	2021-03-25	10.1			Srivastava et al. (2021)
V1405 Cas	23:24:47.73	+61:11:14.8	2021-12-16	10.2	2021-03-30	6.5	Maehara et al. (2021)
V3732 Oph	17:33:14.83	−27:43:11.0			2021-02-15	15.7	Hodgkin et al. (2021a)
V1112 Per	04:29:18.85	+43:54:23.0	2020-11-26	8.9	2021-02-16	14.1	Munari et al. (2020)
V6593 Sgr	17:55:00.00	−21:22:40.1	2020-09-29	11.3			De et al. (2020e)
V1708 Sco	17:23:41.94	−31:03:07.6	2020-09-08	14.4			Kojima & Nishimura (2020)
V1391 Cas	00:11:42.96	+66:11:20.8	2020-07-28	11.7	2020-08-31	11.6	Sokolovsky et al. (2020)
V6568 Sgr	17:58:08.48	−30:05:35.9	2020-07-15	10.6	2020-08-14	16.9	Aydi et al. (2020b)
YZ Ret	03:58:29.55	−54:46:41.2	2020-07-08	6.5	2020-08-19	7.2	Aydi et al. (2020a)
V2029 Aql	19:14:26.30	+14:44:40.2			2020-08-25	14.0	De et al. (2020d)
AT 2020oju	15:25:50.94	−55:10:29.7			2020-07-09	15.9	Kawash et al. (2021a)
V6567 Sgr	18:22:45.32	−19:36:02.2	2020-06-02	13.5	2020-08-18	12.8	De et al. (2020b)
V2000 Aql	18:43:53.33	+00:03:49.4					De et al. (2020c)
V1709 Sco	17:12:00.18	−40:17:56.7	2020-05-10	16.1			Kawash et al. (2020)
V0670 Ser	18:10:42.28	−15:34:18.5	2020-02-23	13.9	2020-02-23	11.5	Aydi et al. (2020d)
V6566 Sgr	17:56:14.04	−29:42:58.2	2020-02-15	12.3	2020-02-20	11.2	Aydi et al. (2020c)
V0659 Sct	18:39:59.70	−10:25:41.9	2019-10-30	9.7			Williams et al. (2019)
V2891 Cyg	21:09:25.53	+48:10:52.2	2019-10-21	15.6	2019-10-07	12.7	De et al. (2019)
V1707 Sco	17:37:09.54	−35:10:23.2	2019-09-14	13.2	2019-09-15	10.1	Strader et al. (2019b)
V3730 Oph	17:38:31.82	−29:03:47.1	2019-09-12	16.6[a]	2019-09-14	12.3	Aydi et al. (2019a)
V3890 Sgr	18:30:43.29	−24:01:08.9	2019-08-27	8.5	2019-09-11	10.5	Strader et al. (2019a)
V0569 Vul	19:52:08.25	+27:42:20.9			2019-08-24	13.5	Aydi et al. (2019d)
V2860 Ori	06:09:57.45	+12:12:25.2	2019-08-18	12.9	2019-08-19	11.6	Aydi et al. (2019c)
V3731 Oph	17:38:34.83	−25:19:04.8	2019-07-12	13.4			De et al. (2020a)
V1706 Sco	17:07:34.17	−36:08:23.2	2019-05-13	13.1			Aydi et al. (2019b)
N Aql 2019	19:03:14.95	+01:20:28.2			2019-04-06	16.2	De et al. (2021d)

Note. List of all spectroscopically confirmed Galactic novae discovered between 2019 and 2021. The names and positions are taken from Koji's List of Recent Galactic Novae and AAVSO's VSX. For both ASAS-SN and Gaia, the date of first detection t_0 and the peak brightness are listed. If no values are listed, it was not detected by that survey.

[a] Though V3730 Oph was detected by ASAS-SN, it was not flagged and reported in the transient pipeline (likely because it was faint), so it is not included in the ASAS-SN discovery rate.

Galactic latitude ($b > 4°$) or those with small measured outburst amplitudes (amp. < 5 mag) are unlikely to be missed Galactic novae (Kawash et al. 2021e). If the quiescent or historic magnitude is too faint to be detected by Gaia, we do not make a cut on the amplitude. We eliminated those at high latitude and those with small amplitudes, and the number of candidates decreased to 435. The bright candidates ($G < 14$ mag) have all been classified, with 9 out of the 12 transients being classified as classical novae. The faint candidates ($G > 14$ mag) include six additional confirmed and highly reddened classical novae, but there are also many unclassified transients. In the absence of extinction, an intrinsically faint nova with peak absolute magnitude $M_G = -5$ mag at a large Galactic distance of 20 kpc would peak at an apparent magnitude of $m_G = 11.5$, so the faint ($G > 14$ mag) nova candidates will all be heavily extinguished and appear red. Most reported transients also include a low resolution ($R \sim 100$) and uncalibrated (in wavelength and flux) BP/RP spectrum, a tool that has proven to be crucial in identifying highly reddened nova candidates. We examined the spectra of the remaining unclassified candidates to identify any transient with a majority of its flux in the red *RP* filter or with strong emission lines. This identified five highly reddened Galactic plane transients detected between 2019 and 2021 with no spectroscopic follow-up.

We obtained spectra of these candidates using the Goodman spectrograph (Clemens et al. 2004) on the 4.1 m Southern Astrophysical Research (SOAR) telescope to look for evidence of past nova eruptions. We detected spectral features in Gaia20dfb and Gaia21dwe consistent with past nova eruptions (Kawash et al. 2021a) and list them as confirmed novae in

Table 2
Unconfirmed Classical Nova Candidates 2019–2021

Name	RAJ2000 (h m s)	DEJ2000 (° ′ ″)	ASAS-SN t_0 (yyyy-mm-dd)	ASAS-SN Peak (g mag)	Gaia t_0 (yyyy-mm-dd)	Gaia Peak (G mag)	Reference
Gaia21axf	17:34:38.07	−31:08:00.1			2021-02-16	18.2	Kawash et al. (2021a)
Gaia20dfc	15:22:33.52	−55:59:40.4			2020-07-09	14.9	Kawash et al. (2021a)
Gaia20btn	17:50:19.43	−31:07:37.9			2020-04-11	18.7	Kawash et al. (2021a)
ASASSN-19pw	18:31:05.75	−14:47:52.6	2019-06-22	15.5			Kawash et al. (2021e)
ASASSN-19nf	14:19:35.09	−59:58:24.0	2019-05-13	16.1			Kawash et al. (2021e)
ASASSN-19fd	17:03:19.29	−29:52:23.3	2019-03-05	13.6			Kawash et al. (2021e)
ASASSN-19am	09:30:39.31	−54:47:04.3	2019-01-08	16.3			Kawash et al. (2021e)

Note. The same columns as in Table 1 for reported transients between 2019 and 2021 that could have been novae but have no spectroscopic detections. All of these transients are near the Galactic plane, so they could be luminous enough to be novae at a reasonable distance with moderate extinction. The Gaia candidates all appear reddened in their BP/RP spectra, but no color information is available for the ASAS-SN transients. Through extensive searches performed in each survey's database, we assume that these candidates are all of the potential unconfirmed Galactic novae between 2019 and 2021. These candidates are given 50% weight compared to the spectroscopically confirmed novae when calculating the discovery rate.

Table 1. Because the follow-up observations were taken months to years after the eruption and the sources are likely highly extinguished, we did not detect flux from Gaia21axf, Gaia20btn, and Gaia20dfc, but we still consider these transients as Galactic nova candidates and list them in Table 2 because their positions, colors, spectral features, and light curves are all consistent with other classified classical novae. Their colors rule out the most common type of classical nova contamination (dwarf novae; Kawash et al. 2021e), but the chance of contamination from microlensing events, young stellar objects, and Be star outbursts remains. Given the rate of confirmation of other candidates, and in lieu of a more complex contamination model, we assign each of these candidates a 50% probability of being a nova for our Monte Carlo simulations described in Section 3.

We assume that this retroactive search has recovered nearly all of the nova candidates reported by Gaia and that any error in the discovery rate caused by missed nova candidates that were reported will be less than Poisson errors. As seen in Table 1, Gaia reported 7, 8, and 12 confirmed novae in 2019, 2020, and 2021, respectively, with an additional 3 unconfirmed candidates listed in Table 2. Assuming Poisson uncertainty for this sample of ∼28.5 novae yields a mean and standard deviation of the discovery rate of 9.5 and 1.8 yr^{-1}, respectively, when running the Monte Carlo simulation over the years 2019 −2021. The dates listed as "Gaia t_0" in Table 1 are the epoch of Gaia's first detection, which can lag the start of the eruption by weeks to months because of Gaia's nonuniform scanning law.

2.2. ASAS-SN Discovery Rate

The ambitious goal of ASAS-SN to observe the entire night sky daily has provided unprecedented cadence for Galactic observations of transients. ASAS-SN transients are reported publicly to https://www.astronomy.ohio-state.edu/asassn/transients.html. In 2018, ASAS-SN switched from observing in V band to exclusively observing in g band. To allow time for deep g-band reference images to be built, we only calculate the discovery rate between 2019 and 2021. Over this time period, we inspected all the ASAS-SN data for confirmed Galactic novae and found that 26 novae were detected in the transient pipeline. If there is no ASAS-SN value for t_0 or peak brightness listed in Table 1, the nova was too highly reddened and therefore too faint ($g \lesssim 18.5$ mag) to be detected by ASAS-SN. V3730 Oph was detected at $g = 16.6$ mag but was never flagged in the pipeline as a transient (fainter transients have a smaller chance of being reported relative to brighter ones; see Equation (4)). We therefore do not include it as a nova in the ASAS-SN discovery rate. Kawash et al. (2021e) found that there were four more reported cataclysmic variable (CV) candidates in 2019 that could be luminous enough to be novae if they are distant enough to be significantly obscured by dust extinction. As with the Gaia candidates, we make the simple assumption that these four candidates, listed in Table 2, have a 50% probability of being classical novae and assume that these were the only potentially missed candidates over this time period. Hence, over the 3 yr considered here, there were 26 confirmed and 4 unconfirmed novae, for a total population of 28 novae. Assuming Poisson statistics yields a mean and standard deviation of the ASAS-SN discovery rate of 9.3 and 1.8 yr^{-1}, respectively.

2.3. The Joint ASAS-SN and Gaia Discovery Rate

If we combine both surveys and account for overlapping discoveries, there were a total of 39 confirmed classical novae and 7 additional candidates detected between 2019 and 2021. This yields a mean and standard deviation of the discovery rate of 14.2 and 2.3 yr^{-1}, respectively. While this observed nova rate is still far below most predictions, it is still the highest *observed* Galactic rate ever used to infer the total nova rate.

3. Monte Carlo Simulations

Our work attempts to repeatedly answer this basic question: if a nova erupted at a specific time and location in the Galaxy, would it be detected and reported as a transient by ASAS-SN and/or Gaia? This idea is expanded to a large sample of simulated novae to estimate what fraction of the Galaxy's novae these surveys detect. By implementing a Monte Carlo analysis, we derive the most likely Galactic nova rate and accompanying uncertainty based off of ASAS-SN and Gaia observations and the uncertainty in the model parameters.

3.1. Positions

The positions of the model novae in the Galaxy are derived by assuming that they trace the stellar mass density of the Galaxy. The stellar density model is outlined in the appendix of Kawash et al. (2021d) and includes a thin disk, thick disk, and halo component as described in Robin et al. (2003) and a two-

component, elongated, triaxially symmetric bulge from Simion et al. (2017). The ratio of the disk mass to the bulge mass, and therefore the ratio of disk to bulge novae assuming equal production per stellar mass, is 1.7. For each run of the Monte Carlo simulation, we randomly pick 1000 nova positions from a possible 10,000 positions. Because this study requires light curves to be generated in each survey at every position, we limit the total number of possible positions to 10,000. In Kawash et al. (2021d), we explored how sensitive the derived nova rate is to the stellar density model, where it was found to change results by ∼15% for the ASAS-SN rate, subdominant to other uncertainties in our calculation.

3.2. Peak Apparent Magnitude

The peak absolute magnitude of each nova is assigned by randomly sampling a normal distribution, described with a mean and standard deviation of $M_{g,G} = -7.2 \pm 0.8$ mag (Shafter 2017). This distribution was measured from M31 novae, and classical novae in the Galaxy could have a different luminosity function (Shafter et al. 2009; Özdönmez et al. 2018). For example, observational biases could suppress the number of bright and faint novae owing to the variable surface brightness of M31. As a test of the effect of changing the luminosity function, we also perform this analysis after doubling the variance to $\sigma = 1.6$ mag. This resulted in a <10% increase in the derived rates, leading to the conclusion that our results are not significantly sensitive to the assumed luminosity function.

The extinction along the line of sight to each nova position is calculated from the `mwdust` package (Bovy et al. 2016). We use the `combined19` version of this extinction model, which is built by combining the Marshall et al. (2006) map of the inner Galactic plane, the Green et al. (2019) map of the northern hemisphere, and the Drimmel et al. (2003) map of the southern hemisphere. The various maps take precedence over each other where they overlap in the order they were listed above. The vast majority of the model novae (95%) lie in the Marshall et al. (2006) map region of the sky. For ASAS-SN, we query the extinction in the Sloan Digital Sky Survey (SDSS) g band, as it is the most similar to ASAS-SN's g-band filter. Extinction in the broad Gaia G-band filter is not directly accessible in `mwdust`, so we estimate this value by first querying the extinction in the SDSS g and i bands. The relationship between these SDSS filters and Gaia's G-band filter was fit to a third-order polynomial with the form

$$G - g = -0.1064 - 0.4964x - 0.09339x^2 + 0.004444x^3, \quad (1)$$

where $x = g - i$ (Gaia Collaboration et al. 2021).

An additional concern when estimating the extinction for a model of Galactic novae is that the 3D dust maps that comprise the `mwdust` package only estimate the extinction out to distances where the colors of stars can be measured, and therefore they do not extend to the largest Galactic distances and the highest extinction regions. If a model nova is beyond the largest distance bin of `mwdust`, we add extinction by fitting the amplitude of the extinction along a line of sight and assuming that the dust is described with an underlying double exponential distribution that is a function of Galactic radius and height from the plane. We use $(r_0, z_0) = (3.0, 0.134)$ kpc for the scale length and height, respectively (Li et al. 2018). The amount of extinction is fit out to the distance where `mwdust` has information, and then we use the results to extrapolate to the nova distance. For 55% of simulated novae, `mwdust` extends to the distance of the nova, so no extinction is added. For those remaining novae beyond the 3D dust maps, the mean extinction added in the g and G bands is 0.9 and 0.6 mag, respectively, and the median extinction added in the g and G bands is 0.1 and 0.7 mag, respectively. The distributions of the estimated extinction before and after this correction are shown in Figure 2. The median nova will experience ∼10 mag of extinction in g band and ∼6 mag of extinction in G band.

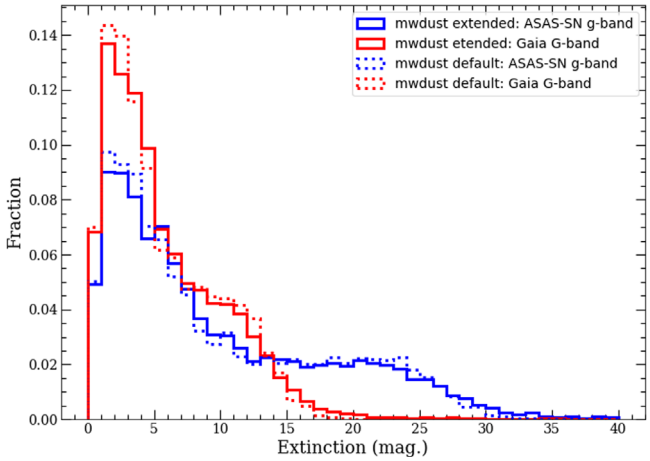

Figure 2. The normalized extinction distributions of 10,000 simulated novae in the ASAS-SN g-band filter (blue) and Gaia G-band filter (red). These distributions are estimated from the `mwdust` package (default values shown as dotted lines), and we add additional extinction if the line of sight is not complete out to the distance of the nova (solid line).

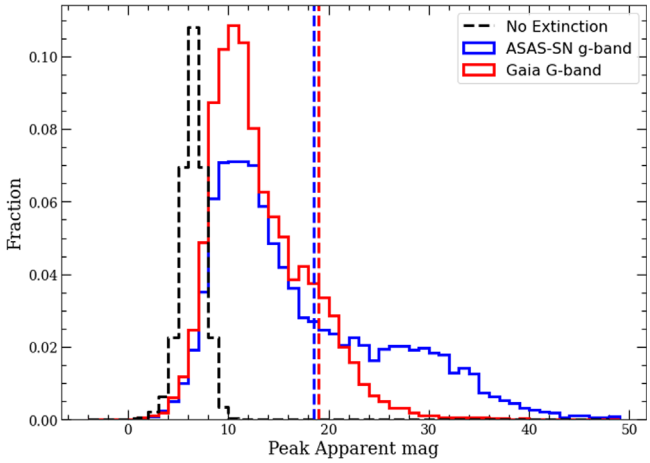

Figure 3. The normalized distributions of peak apparent magnitude of 10,000 simulated novae in the g-band filter (blue) and G-band filter (red) The dashed vertical lines indicate the limiting magnitude of ASAS-SN (blue) and Gaia (red). Also shown is the distribution with zero extinction with the peak scaled to fit (black dashed line). This demonstrates that dust is a much larger factor than the luminosity or distance in determining the peak apparent magnitude of a nova.

With the peak luminosity, the distance, and the extinction in g and G bands estimated, the peak apparent magnitude of each model nova can be calculated using the distance modulus. The results are shown for 10,000 model novae in Figure 3. The differences between the Gaia and ASAS-SN peak apparent magnitude distributions are entirely due to the different observing filters used; the bluer ASAS-SN g band is more vulnerable to extinction from interstellar dust compared to the

broader Gaia G band. This figure shows that extinction is the largest factor in determining the apparent brightness of a Galactic nova. The dashed black distribution ignores extinction, and therefore its variance is caused by variations in the luminosity and distance of a nova; in this case, the standard deviation in the peak apparent brightness is only 1.2 mag. However, when considering extinction, the standard deviation of the peak brightness seen in Gaia's G-band filter is 5.0 mag, and in ASAS-SN's g-band filter the standard deviation is 8.8 mag. Based only on the peak brightness, ∼90% of Galactic novae are bright enough to be detected by Gaia ($G < 19$ mag), compared to the only ∼60% detectable by ASAS-SN ($g < 18.5$ mag).

3.3. Light Curves

The modeling work to derive the apparent magnitude distribution of Galactic novae was largely laid out in Kawash et al. (2021d), but the detection efficiency in the survey data was only broadly estimated. Here we incorporate the model into each survey's data to more accurately estimate the detection efficiency. Each simulated nova is given a random eruption date between 2019 January 1 and 2021 December 31. While in principle novae first discovered at the start of our survey period (2019 January) could have exploded in 2018, and hence outside of our simulation, the predicted and observed number of novae in the first half of January is so low that this potential issue does not have a meaningful ($\lesssim$1%) affect on our results. Though not entirely symmetric, this effect is also diminished by novae that erupt near the end of the simulation in late 2021 that would be discovered in 2022, after the end of the simulation.

The temporal evolution of the brightness is modeled by sampling a distribution of nova speeds and then constructing the full shape of the light curve from a sample of known nova light curves. We used 93 AAVSO V-band nova light curves from Strope et al. (2010) and 75 Stony Brook/SMARTS V-band light curves from Walter et al. (2012) as light-curve templates. V band was chosen because it was the most well-sampled filter from the two databases and also close to the g and G bands of ASAS-SN and Gaia. Motivated by the typical intrinsic colors of novae (e.g., van den Bergh & Younger 1987) and the fact that extinction is the key factor in determining the apparent brightness (not the luminosity), we assume a flat spectrum ($V_{\rm peak} = g_{\rm peak} = G_{\rm peak}$) when transforming these templates to g and G bands.

Previous completeness studies have used several methods to estimate how long a nova is detectable, including defining a discrete number of observable days after eruption (Mróz et al. 2015) and assuming a linearly declining light curve (De et al. 2021b). By using real light curves as templates, we do not have to make simplifying assumptions about the shape of the light curves, which can be quite complex (Strope et al. 2010). However, we also carry out the analysis by using linearly declining light curves to explore how sensitive the results are to this property, and we discuss the results in Section 5.2.

We took additional steps to reduce errors in the light-curve templates. A template should only include flux from the nova eruption and not from when the nova has returned to the quiescent state or from nearby background stars. Most of the quiescent magnitudes are listed in Table 1 of Strope et al. (2010) for the novae presented in that work, so we truncate the light curve once it declines to within 3 mag of this quiescent magnitude. Walter et al. (2012) note that there are cases in the SMARTS sample of novae when the fading remnant becomes blended with a background star, and from inspecting these light curves, this does appear to be true in a few cases. We also cut off light curves within a magnitude of any prolonged plateaus many magnitudes below maximum to eliminate this contamination. If the duration of the template light curve is shorter than the survey length, we extend the template by assuming that it will decline linearly at the average pace of the light curve.

Each nova is randomly assigned a decline speed by sampling a lognormal distribution for t_2 (the time it takes a nova to decline 2 mag from peak) with mean and standard deviation equal to 18.7 and 3.2 days, respectively, based on modeling of observed novae and accounting for selection effects (Kawash et al. 2021e).

There has been a large effort to establish novae as standard candles. The relationship between the luminosity and the speed of a nova, commonly referred to as the maximum magnitude versus the rate of decline (MMRD) relation, was once thought to be a tight correlation (Capaccioli et al. 1989; della Valle & Livio 1995), but in recent years many examples of novae that do not follow the published relationships have been found, especially those that are fainter and faster (Kasliwal et al. 2011; Shara et al. 2017a). These faint, fast novae have been suggested to be a reason for a factor of three discrepancy in extragalactic nova rate estimates (Shara et al. 2016). In our primary model, we assume that the luminosity of a nova simply sets an upper bound on the speed or t_2 value. Put another way, the luminous novae are restricted to having small t_2 values, but the fainter novae are allowed all values of t_2. The boundary between the forbidden and allowed values is shown as a blue dashed line in Figure 4, with the allowed values being below this line. Any model nova with a given luminosity that is assigned a forbidden t_2 value has this parameter resampled until an allowed value is found. This forbids luminous, slow novae, as no such example has been found, but allows for any number of faint, fast novae.

The maximum magnitude versus rate of decline for 10,000 model novae is shown in Figure 4. The distribution of t_2 is discontinuous because of the discrete t_2 values of the template light curves. Also shown on this plot is the MMRD correlation measured in della Valle & Livio (1995; the red shaded region), real Galactic nova values measured from "Gold" and "Silver" Gaia distances (denoted as the green stars; Schaefer 2018), and various extragalactic novae (Kasliwal et al. 2011; Shafter et al. 2011; Shara et al. 2016). The faint, fast novae are arguably overrepresented in our model compared to observations, so we also rerun the analysis by treating MMRD as a strict correlation and discuss the results in Section 5.2. We explored the detection efficiency of each survey in this parameter space (see Sections 3.4 and 3.5 for details on detection efficiency), and the results are shown in Figure 5. Though faint, fast novae are clearly harder to detect in the model, the difference in the recovery fraction of faint, fast novae compared to novae that adhere to the MMRD relation is no more than a factor of two. This means that it is unlikely that a large population of faint, fast novae exist in the Galaxy that have not been detected by all-sky surveys, unless such novae have a very different spatial distribution and are more embedded in dust than typical novae.

Once each model nova is given a decline rate, we assign a light-curve template by finding the Strope et al. (2010) or

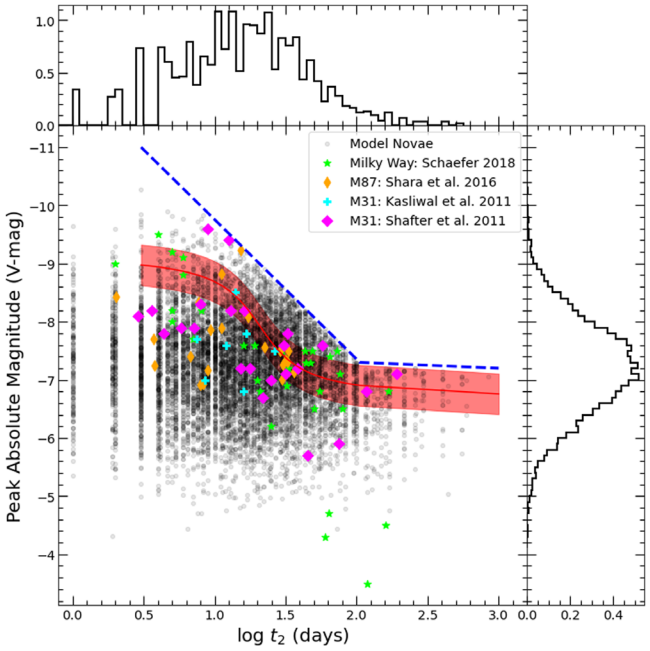

Figure 4. Distribution of the peak absolute magnitude vs. time to decline by 2 mag from maximum (t_2) for 10,000 model novae (black circles). The peak absolute magnitudes are sampled from a normal distribution, and the t_2 values are sampled from a lognormal distribution. The patchiness in the t_2 distribution is the result of a limited number of nova light-curve templates. The allowed values in this parameter space are shown below the blue dashed line, and this is compared to real Galactic nova values estimated from Gaia distances (Schaefer 2018; denoted with green stars), extragalactic measurements (pink diamonds, cyan crosses, and orange diamonds; Shafter et al. 2011; Kasliwal et al. 2011; Shara et al. 2016), and the MMRD correlation derived in della Valle & Livio (1995; shown as the red shaded region).

Walter et al. (2012) light curve closest to the randomly assigned t_2 value. The template is then scaled to the assigned peak apparent magnitude. The model novae now have all of the information needed to inject them into the survey data, and next we discuss how that is performed for each survey.

3.4. Gaia Simulation

For each nova position we used the Gaia Observation Forecast Tool[16] to provide the epochs at which Gaia observed the location, and we assume a fixed detection threshold of $G < 19$ mag. We then sample the template light curve at the cadence of Gaia, and several examples are shown in the right column of Figure 6. We draw the noise in the light curve from a normal distribution with standard deviation

$$\sigma = 3.43779\ \text{mag} - (G/1.13759) + (G/3.44123)^2 - (G/6.51996)^3 + (G/11.45922)^4 \quad (2)$$

if 13 mag $< G <$ 19 mag and $\sigma = 0.02$ mag for $G <$ 13 mag.

To determine whether a model nova would be reported by GSA, we start with three basic requirements (outlined in Hodgkin et al. 2021b). First, there need to be detections in both fields of view (FOVs; preceding or trailing) brighter than $G < 19$ mag within 40 days of each other. Second, the detected brightness needs to exceed that of all stars within a 1.″5 radius in Gaia DR2. Third, there cannot be a $G < 12$ mag star within a 10″ radius in Gaia DR2.

[16] https://gaia.esac.esa.int/gost/

Even if a transient satisfies these three requirements, there are additional ways for it to be missed in the pipeline. For example, a single source can have multiple source IDs, ambiguous matches in Gaia DR2, multiple sources within the core region, etc. (Kostrzewa-Rutkowska et al. 2018). It is difficult to determine when this will happen in the simulation, so we make a statistical estimate by looking at the reporting efficiency of novae in Table 1. There are 20 novae reported by GSA that were also detected by other surveys (amateurs, ASAS-SN, PGIR, etc.); however, after further inspection of the Gaia database and the Gaia observation forecast tool, there are seven additional novae (V0569 Sct, V1708 Sco, V5693 Sgr, V1710 Sco, V1674 Her, V0606 Vul, and RS Oph) that should have been reported based on the three major criteria listed above. Hence, GSA reported no more than $20/27 \approx 74\%$ of the novae that passed these criteria, and the true reporting efficiency is likely somewhat lower because of the strong chance of additional candidates that were unreported by other observers. We treat this estimate as a 1σ upper limit with 10% uncertainty, so for each Monte Carlo trial we assign Gaia a reporting probability for novae that pass all of the hard-coded requirements by sampling a normal distribution with mean $\mu = 0.67$ and standard deviation $\sigma = 0.067$. This is necessarily a crude model to summarize the complex process that leads to a candidate nova being reported and undoubtedly an important source of uncertainty in our simulations. Future observations of novae and Gaia alerts can help constrain this reporting efficiency.

3.5. ASAS-SN Simulation

The cadence and limiting magnitude of ASAS-SN observations were calculated by constructing image subtraction light curves without adding the reference flux from the ASAS-SN data at the 10,000 positions of the model novae. This automatically provides a sampling of the cadence, noise uncertainty (due to the lunar cycle and weather conditions), and contamination from bright, nearby stars. The formal photometric uncertainties reported in ASAS-SN light curves tend to underestimate the true uncertainties (Jayasinghe et al. 2018), and this can particularly be true in the Galactic plane owing to crowding, even with the benefits of image subtraction. We estimated a rescaling of the uncertainties for each light curve by looking at the distribution of the ratio f_i/σ_i, where f_i is the flux and σ_i is the reported error in the flux of each camera at each position. If the error estimates are correct, then the standard deviation of this distribution should be unity. When it is larger, we increase σ_i by the factor needed to make the width of the distribution unity. For many of the random nova light curves, the rescaling is large enough to lead to a $\sim$1 mag reduction in sensitivity on average. Because this work is looking at Galactic novae that tend to be located at crowded low Galactic latitudes, these affects are more severe than for an extragalactic supernova study.

When injecting the model nova light curves into the ASAS-SN data, we assume that the nova would be detected if it is brighter than these rescaled 5σ upper limits on each particular epoch. Similar to the Gaia analysis, we fit a polynomial to photometric errors in ASAS-SN data, and we add noise to the light-curve templates by sampling a normal distribution with a

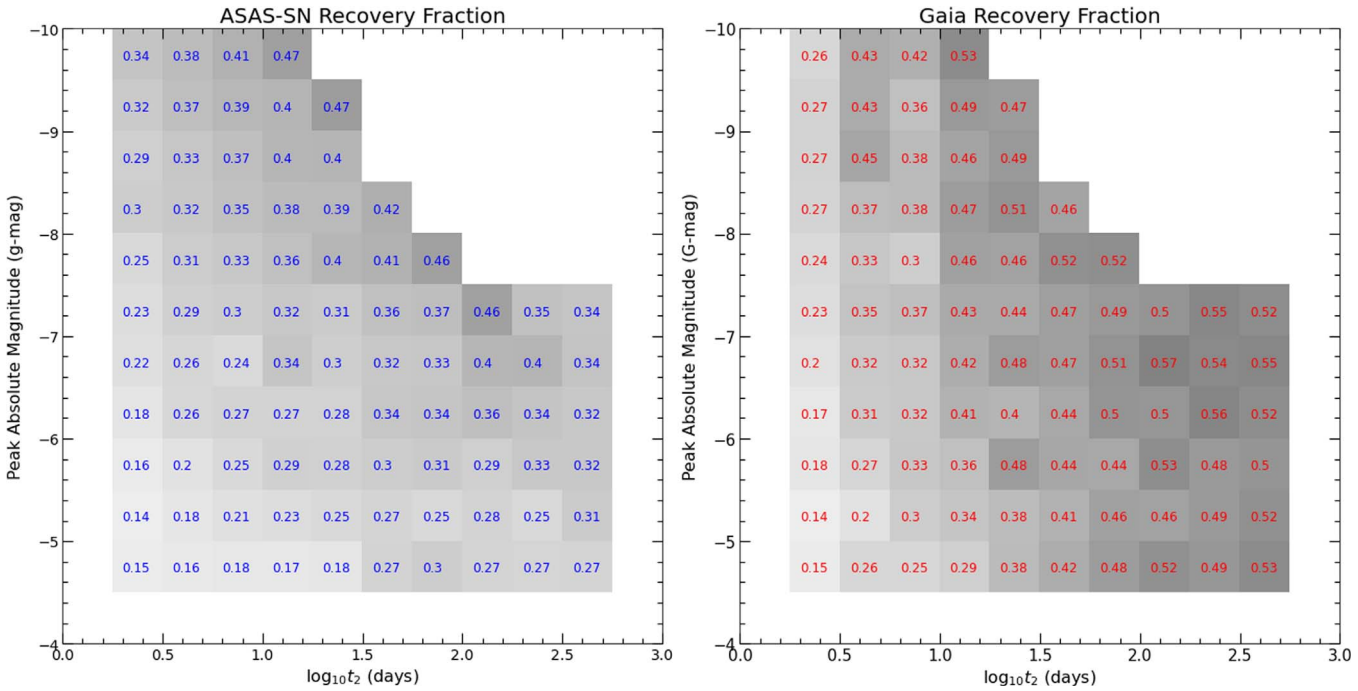

Figure 5. The recovery fraction of model novae in ASAS-SN and Gaia as a function of peak absolute magnitude and t_2. The recovery fraction values are calculated on a grid of 0.5 mag by 0.25 $\log_{10}(t_2)$ days and are shown in each square, with darker gray scale indicating a higher recovery fraction. While novae that adhere to the supposed MMRD relation are on average easier to detect, they are only recovered about twice as efficiently as faint, fast novae, implying that all-sky surveys would have detected a substantial population of faint, fast novae if they were present.

measured standard deviation of

$$\sigma = 0.08\ \text{mag} + 0.04(g-13) - 0.04(g-13)^2/\text{mag} + 0.02(g-13)^3/\text{mag}^2 - 0.002(g-13)^4/\text{mag}^3 \quad (3)$$

if $13\ \text{mag} < g < 18.5$ mag, and $\sigma = 0.02$ mag for any $g < 13$ mag.

When a transient is reported by ASAS-SN, it is cross-checked to catalogs like Gaia and the Panoramic Survey Telescope and Rapid Response System (Pan-STARRS; Chambers et al. 2016) to roughly estimate the outburst amplitude. This helps differentiate classical nova candidates from other CV outbursts, but the large pixel scale of ASAS-SN ($8''$ pixel^{-1}) can lead transients to have underestimated outburst amplitudes when their position is coincident with another star. To account for this, we also require detections to be 5 mag brighter (Kawash et al. 2021e) than the closest star in Gaia DR2 within half an ASAS-SN pixel, to assure that the transient would be recognized as having a large outburst amplitude.

The goal of the ASAS-SN pipeline is to discover previously unknown transients and variable stars. To avoid continually looking at known variables, the ASAS-SN pipeline does not generate candidate images for flux changes detected within 5 pixels of known Mira, long-period, or semiregular variables. A list of the positions, types, and magnitude range of known variables is acquired from VSX and OGLE and is maintained in the ASAS-SN database. We inspect this same list in the simulation and require that the model novae also satisfy this condition. If a transient is near a different type of variable, a candidate image will be generated; however, if a new transient is found near a known one, it is possible for the new transient to be confused with a known repeater and consequently not reported. To incorporate this into the model, a transient has to be a magnitude brighter than the listed magnitude range of any known variable within half an ASAS-SN pixel of the simulated nova.

The last step for a transient that is detected by ASAS-SN to be reported is that a human needs to flag the source in the data as real and previously unreported. As mentioned above, the probability of this occurring scales with the signal-to-noise ratio (S/N). The images of bright candidates ($g < 15$ mag) generate alert emails and are filtered into a pipeline dedicated to finding Galactic classical novae. Fainter Galactic transients are commonly reported by ASAS-SN but with lower completeness due to the number of false positives from artifacts increasing at fainter magnitudes. Generally, the closer a candidate is to the detection limit, the less likely the image is to be vetted by a human and reported as a transient. The probability for a single detection of an extragalactic supernova to be reported in ASAS-SN was studied by D. Desai et al. (2022, in preparation) and found to be

$$\begin{cases} 0.65 & \text{S/N} \geqslant 12 \\ (1 + (\text{S/N} - 12)/7) \times 0.65 & \text{S/N} < 12, \end{cases} \quad (4)$$

where S/N is the signal-to-noise ratio of each detection. In the simulation, each detection that satisfies the above requirements has this probability of being flagged. This detection probability is per individual epoch, so the brighter and slower transients have a much higher likelihood of being reported than the faint and fast ones.

4. Global Nova Rate Estimates

The results of the Monte Carlo simulation show the probability distribution of the global Galactic nova rate based on ASAS-SN and Gaia observations and reporting of Galactic novae between 2019 and 2021. We run the Monte Carlo 1000 times, each time sampling different values for (i) the nova

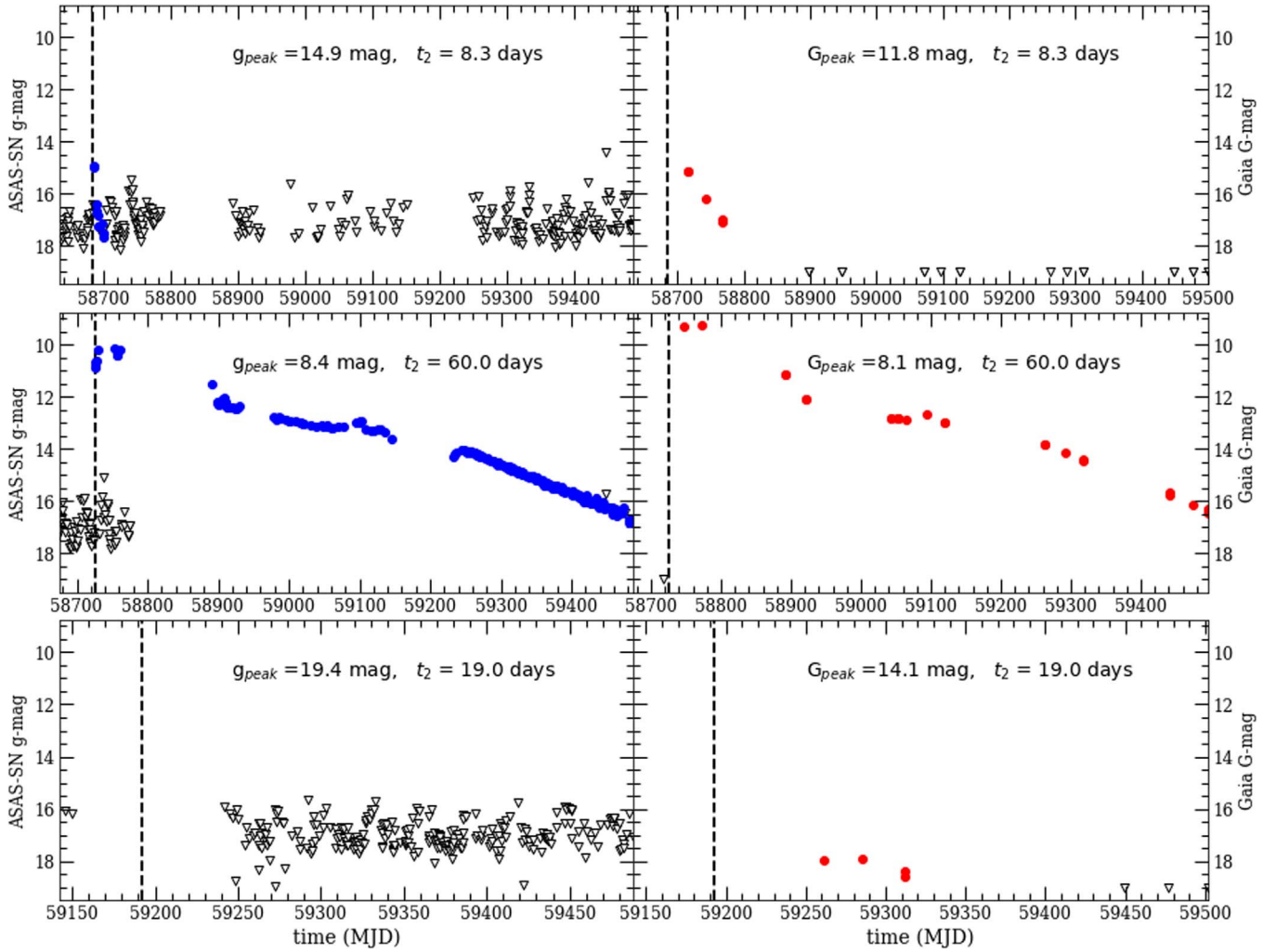

Figure 6. Three examples of simulated novae in ASAS-SN (left) and Gaia (right). The detections are shown in blue for ASAS-SN and red for Gaia, with nondetections shown as black triangles. The epoch of eruption is denoted by the vertical dashed line, and the peak apparent magnitude and t_2 are listed in each panel. The top row shows a fast reddened nova, the middle row shows a nearby and slow nova (the nondetections shortly after the eruption indicate that the transient has saturated the ASAS-SN detectors), and the bottom row shows a reddened nova that was only detected by Gaia.

positions, (ii) the light curves' speed and shape, (iii) eruption dates, (iv) peak luminosities, (v) the probability of detected transients being reported, and (vi) the discovery rates based on Poisson sampling. The Galactic nova rate is then calculated for each trial by dividing the discovered rate by the estimated recovery fraction for each respective sample. Each trial provides a different estimate of the Galactic nova rate, and we take the median rate as the most likely and 68.2% of the width as the 1σ uncertainty. The results of the Monte Carlo simulation are shown in Figure 7.

We simulate the Gaia and ASAS-SN surveys individually and as a joint search, providing three estimates of the Galactic nova rate. The joint estimate might appear to be redundant with the former two, but the fraction of novae discovered by neither, one, or both surveys provides additional information not captured in the prediction from a single survey since the surveys have different filters and cadences. The three rates are all consistent at the 1σ level: ASAS-SN, Gaia, and the combination of both surveys predict global Galactic nova rates of 28^{+6}_{-6} yr^{-1}, 22^{+5}_{-4} yr^{-1}, and 26^{+5}_{-4} yr^{-1}, respectively. These results suggest that the two surveys combined detected ∼54% of the Milky Way's classical nova eruptions that occurred between 2019 and 2021, a much higher recovery fraction than recently estimated (Özdönmez et al. 2018; De et al. 2021b). Individually we estimate that the recovery fraction of ASAS-SN is ∼33% and the recovery fraction of Gaia is ∼42%.

Breaking those estimates down further, for ASAS-SN, about 40% of novae are too faint for discovery because they are too highly extinguished, an additional ∼20% are lost because there is not an observation while the nova is brighter than the average detection limit of $g < 17$ mag (largely from seasonal gaps), and the last ∼7% are lost because of various pipeline features (low S/N, confusion, avoiding known variables, etc.). This is a lower fraction of novae lost because of cadence and the pipeline than the assumption of 40% used in Kawash et al. (2021d), so the nova rate derived in that work was overestimated.

For Gaia, only ∼14% of novae are too faint because they are too highly extinguished, ∼12% are lost because of lack of cadence, and ∼35% are lost because of various pipeline features (requiring detections in both FOVs, source confusion, etc.). This is consistent with the analysis of extragalactic supernovae that found that the scanning law and the need to minimize the false-alarm rate dominate the completeness of GSA (Hodgkin et al. 2021b). Surprisingly, the higher cadence of ASAS-SN loses more novae that peak bright enough for

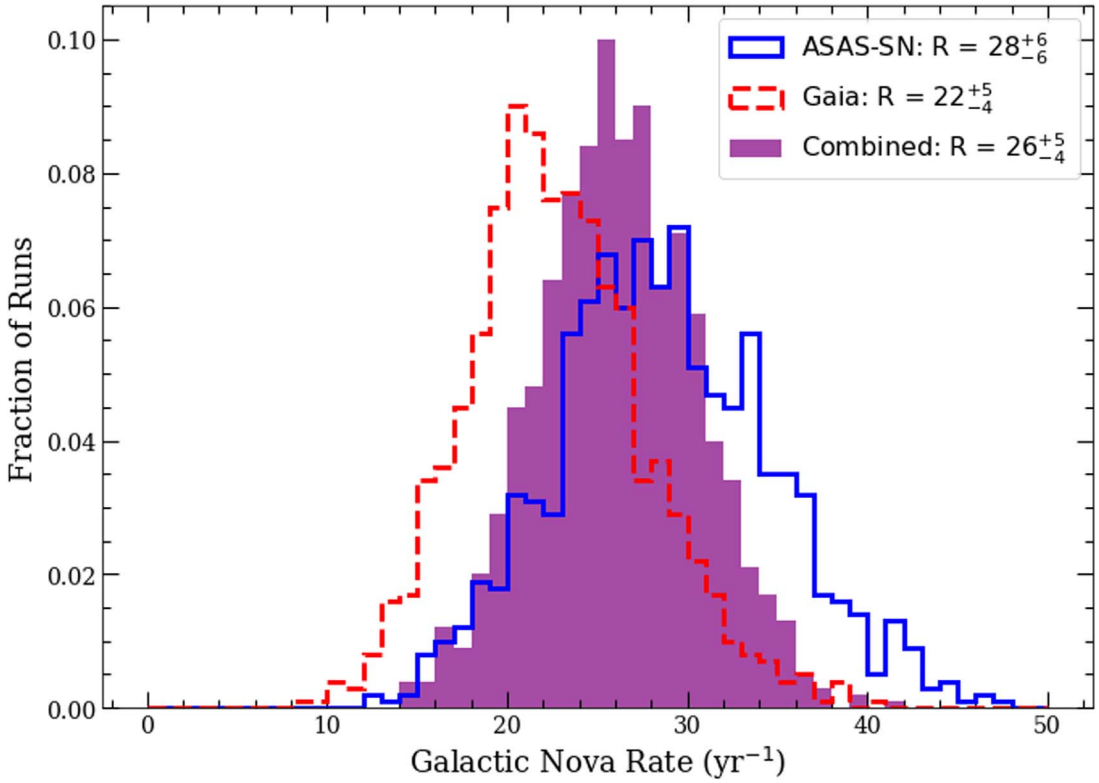

Figure 7. The predicted Galactic nova rate based on 1000 Monte Carlo trials, from ASAS-SN (blue histogram), Gaia (red histogram), and a combination of both surveys (purple histogram). We give the median values of the distributions as the most likely Galactic nova rate and include the 16% and 84% confidence regions. The results are all consistent at the 1σ level, with the most likely rate from both surveys predicting a Galactic nova rate of $R = 26 \pm 5$ yr^{-1}.

detection than Gaia, but this is again because of dust extinguishing novae so that the bluer ASAS-SN observations have a much shorter time for discovery and because ASAS-SN has a lower recovery rate at fainter magnitudes.

To assess the accuracy of the model, we compare the results of the simulation to the real novae in Table 1. Any significant conclusions should be taken with caution because of the small sample size of discovered novae, but this exercise can still shed light on the accuracy of the model. First we look at what fraction of the survey's discovery sample was also discovered by the other survey. In the simulation, about 60% of the ASAS-SN-discovered novae were also discovered by Gaia, compared to the observed value of $14/26 \approx 54\% \pm 14\%$ (assuming Poisson uncertainty) from Table 1. Roughly 50% of the simulated novae discovered by Gaia were also discovered by ASAS-SN, compared to the observed $14/30 \approx 47\% \pm 12\%$ of the real Gaia sample. The overlap in discoveries in the simulation is consistent within uncertainties with that in the real novae.

The sky positions of the simulated and real samples of novae are shown in Figure 8. Again, the degree to which the positions agree is hard to assess because of low number statistics, but there is broad agreement between the distribution of simulated and observed novae. Notably, both the observed and simulated nova populations in the bulge region show more novae at Galactic longitude $l > 0°$ than at $l < 0°$. This is likely due to the elongated bulge ("bar") in this region of the Galaxy, which places typical novae at $l > 0°$ at closer distances, and behind less dust, than those at $l < 0°$.

The apparent exception to the agreement between model and data is in the southern region of the Galactic plane, where no novae were observed between an R.A. of 8 and 14 hr from 2019 to 2021. This could suggest a bias against discovering plane novae in the south compared to the north, which would not be expected given that both ASAS-SN and Gaia are all-sky surveys. This discrepancy could also primarily reflect small number statistics, since in 2017 and 2018, just before the time span of this survey, several novae in this southern plane region were indeed discovered (V906 Car, V357 Mus, V549 Vel, V1405 Cen), which would tend to equalize the statistics.

In addition to comparing where novae are found, we also looked at when novae are discovered by the surveys. Although the simulated novae are given random eruption dates uniformly between 2019 and 2021, we do not expect them to be discovered uniformly throughout the year owing to annual changes in observing conditions. When the novae are first detected by ASAS-SN and Gaia in our models is shown as histograms in Figure 9, along with the observed first detections of novae from Table 1 with 1σ Poisson errors. From November to January, the Galactic center region is behind the Sun, and therefore much of the Galaxy is not observable. In February, this field becomes observable again and the novae still bright enough for detection can be discovered, resulting in our model predicting this month to have the highest discovery rate for ASAS-SN and one of the highest for Gaia. These are the only pronounced patterns in the predicted annual discovery rate of ASAS-SN. The satellite observations of Gaia also have a second area of avoidance around solar opposition (see Figures 4 and 5 of Gaia Collaboration et al. 2018). This causes an annual pattern of two Gaia nova discovery seasons lasting roughly 3 months, with over half of first detections happening in February and August when the Galactic center comes out of the areas of avoidance. The ASAS-SN and Gaia detections track relatively well with the model predictions but with large

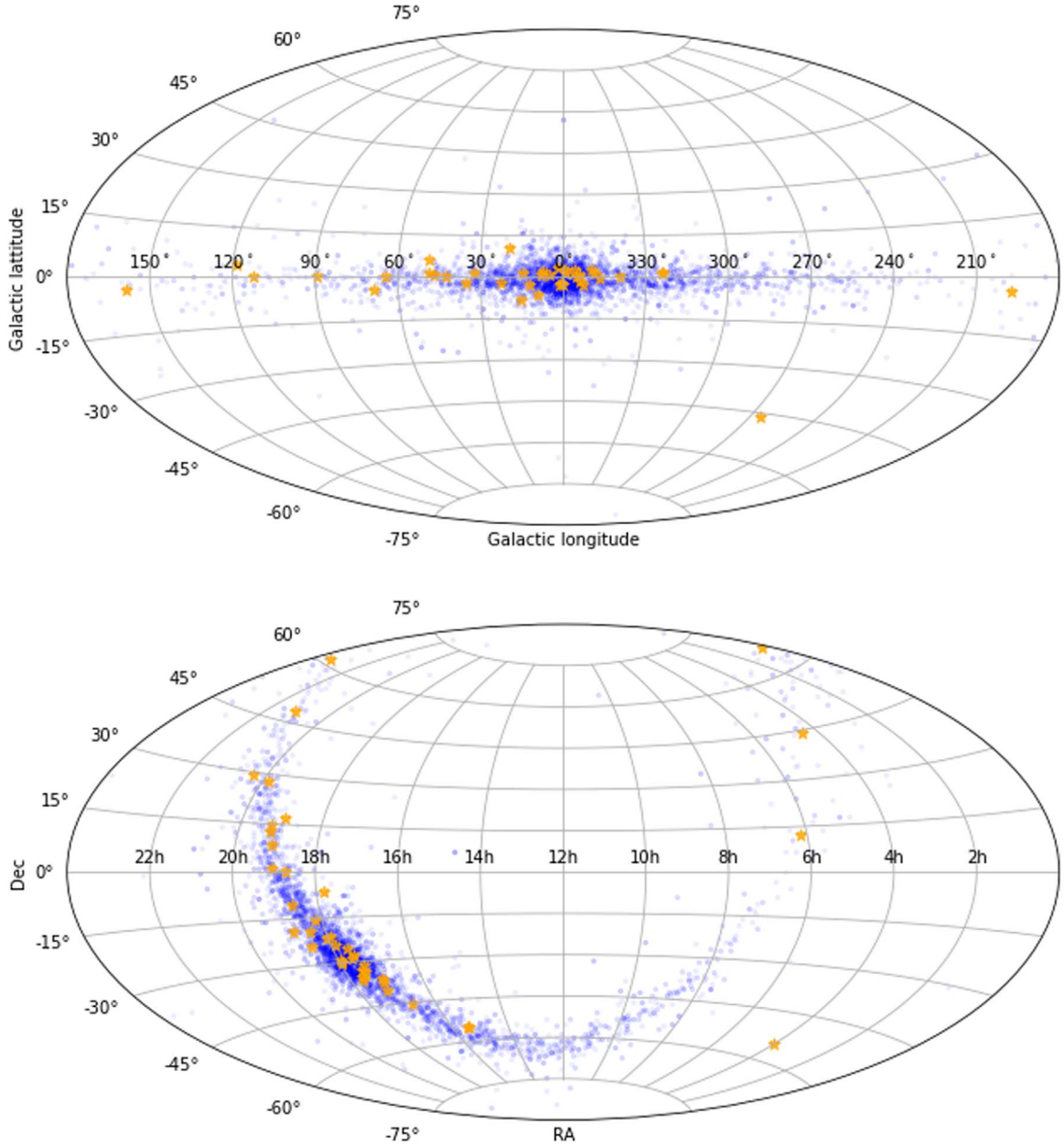

Figure 8. The positions of simulated novae that are discovered in our model (blue circles) compared to the real sample discovered between 2019 and 2021 (orange stars). The simulated positions are derived assuming that novae trace the stellar density of the Galaxy. The elongated bulge, oriented at a roughly 20° angle from the Sun–Galactic center line, appears to place more recoverable bulge novae at $l > 0°$ compared to $l < 0°$.

uncertainty because of the small number of novae per monthly bin.

5. Comparisons to Previous Results

Our predicted rate of 26 ± 5 yr^{-1} is notably lower than most recent direct Galactic nova rate estimates (see Figure 1). All of the estimates in Figure 1 are consistent within 3σ, largely because of the relatively large uncertainties, and the following discussion is focused on identifying any systematic errors that could bring these estimations into better agreement. The rate derived in this work has relatively small error bars compared to the other estimates because the nova sample used to directly extrapolate the global rate is the largest sample of novae used to date and because our model suggests a higher recovery fraction resulting in smaller variance between Monte Carlo trials.

Our derived rate is perhaps consistent with the naked-eye nova direct extrapolation rate of 50^{+31}_{-23} yr^{-1} (Shafter 2017), but mostly due to the latter's large uncertainty. It is inconsistent at the 1σ level with the rescaled (because of faint, fast novae) M31 inferred Galactic rate of $\sim$50−70 yr^{-1} from the same work.

5.1. Bulge versus Disk Rates

In our primary model, we assume that novae occur in proportion to the stellar mass in both the bulge and disk. Because roughly 40% of the novae are in the bulge region ($R < 3$ kpc) compared to the 60% of novae that would be considered to be in the disk ($R > 3$ kpc), this predicts a bulge and disk rate of $\approx 10 \pm 2$ yr^{-1} and $\approx 16 \pm 2$ yr^{-1}, respectively. There is an independent estimate of the bulge nova rate from

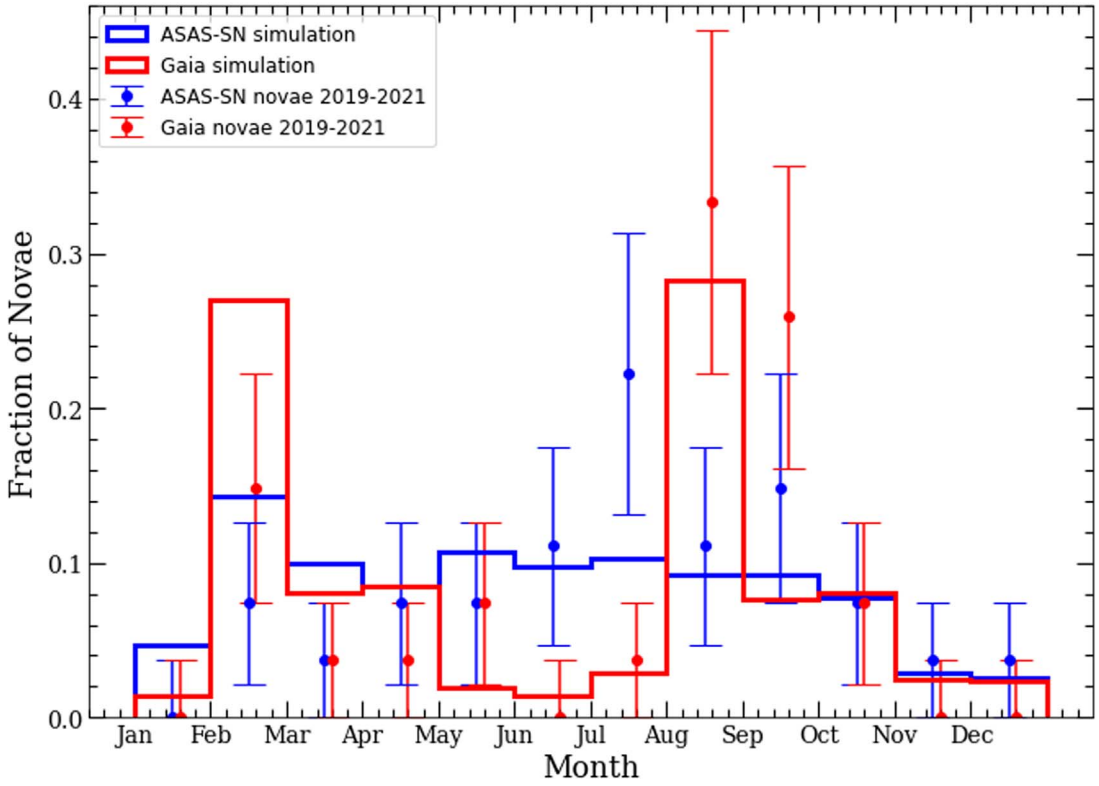

Figure 9. Comparison of the month of first detections of model novae (solid histograms) vs. discovered samples (scatter points with Poisson error bars). Both surveys have a seasonal gap while the Sun is in Sagittarius from November to January, and Gaia (shown in red) has an additional seasonal gap 6 months later because of the rotation direction of the satellite. When a field comes out of solar constraint, the model predicts an excess of nova discoveries.

the OGLE-IV survey, of 13.8 ± 2.6 yr^{-1} (Mróz et al. 2015), which is just over 1σ higher than our value.

We find little difference ($\lesssim$10%) in the detection efficiencies between the bulge and disk in our work, with ASAS-SN predicted to recover ∼37% of disk novae and ∼28% of bulge novae, and Gaia recovering ∼43% of disk novae and ∼40% of bulge novae. This means that our inferred total Galactic nova rate would not meaningfully change for reasonable differing assumptions about the bulge and disk populations of novae (Kawash et al. 2021d). As an example, Shafter & Irby (2001) estimated that the M31 nova rate per unit luminosity of the disk was 0.4 that of the bulge. Assuming a similar ratio for the mass in our model yields bulge and disk rates of $\approx$15 and $\approx$11 yr^{-1}, respectively. Hence, even a mild enhancement of the bulge nova rate with respect to the disk nova rate could bring our results into full agreement with the OGLE-IV results, but as stated above, the disagreement is small even with our standard model.

Our inferred rate of disk novae is not consistent even at the 2σ level with the average disk rate estimate of 67^{+21}_{-17} yr^{-1} from Özdönmez et al. (2018). This rate was derived from an estimate of the local (within 1–2 kpc) nova population extrapolated to the entire disk. The origin of the disagreement is not immediately clear but could potentially arise if the distances to some of the novae in their sample were underestimated.

5.2. Comparison to Palomar Gattini-IR

The rates derived in this work are perhaps most easily comparable to the PGIR estimate of 44^{+20}_{-9} yr^{-1} (De et al. 2021b), the only other direct Galactic estimate made from a systematic large (though not all-sky) time-domain survey. However, the PGIR rate is substantially higher than those derived here, with the overlap in the posterior distribution functions <20%. Here we assess whether the discrepancy can be explained by different assumptions between the two models.

Kawash et al. (2021d) explored the sensitivity of the ASAS-SN-derived nova rates to various model assumptions and found that the rates are most sensitive to the assumed extinction law ($A_V/A_{K_s} = 13.44$ vs. $A_V/A_{K_s} = 8.65$; Nataf et al. 2016) and the stellar density model used to distribute the nova positions (Robin et al. 2003 vs. Cautun et al. 2020). Because a steeper reddening law increases the g-band extinction and the Cautun et al. (2020) stellar density model places more novae closer to the plane (see Figure 1 of Kawash et al. 2021d), the recovery fraction of novae in ASAS-SN decreases, resulting in a 33% increase in the derived rate. Assuming a similar increase for this work would increase the ASAS-SN derived Galactic nova rate to $R \approx 37$ yr^{-1}, still consistent with our primary model at the 2.2σ level and now consistent with the PGIR rate at the 1σ level. However, the Gaia rate is much less sensitive to these changes, as it is better at finding extinguished novae in the plane, so a significant discrepancy between the Gaia and PGIR rates would remain.

As seen in Table 1 of Kawash et al. (2021d), the PGIR predicted rate is not sensitive to changes in the distribution of positions, extinction model, or bulge-to-disk ratios of novae. Those rates were derived assuming a detection efficiency of 17%, estimated from the completeness study of PGIR data (De et al. 2021b).

Arguably the largest difference between the PGIR study and this work is the assumed shapes of nova light curves and the adherence to the MMRD relation. We assume that the distribution of speed class is derived from the lognormal

distribution of t_2 measured in Kawash et al. (2021e) and then use a real nova light curve with the closest value of t_2 as a template to model the fading from maximum light. De et al. (2021b) use the peak luminosity to find the corresponding t_3 value using the MMRD relationship measured in Özdönmez et al. (2018) and then assume that the apparent magnitude will fade linearly in time. We reran our analysis, this time using the PGIR method to derive the light-curve speed and shape, to see whether this could explain the discrepancy in the results. This led to a small decrease in the derived rates, with the ASAS-SN, Gaia, and joint rates changing to 26 ± 5 yr^{-1}, 21 ± 5 yr^{-1}, and 24 ± 4 yr^{-1}, respectively. This minor decrease is because the MMRD relation measured in Özdönmez et al. (2018) maps the average nova luminosity of $M = -7.2$ mag to a relatively slow decline $t_3 \approx 73$ days, and the strict adherence to the MMRD relation does not allow for faint and fast novae. This makes novae observable for a slightly longer period of time compared to the method used in this work. But overall, the differences in the shape of the simulated nova light curves cannot explain the inconsistencies in the results.

One of the three major requirements for a nova candidate to be identified in the PGIR pipeline is that the transient has to be 3 mag brighter than any 2MASS counterparts within a radius of 10″ (De et al. 2021b). From the positions and peak brightness of PGIR-detected novae listed in Table 1 of De et al. (2021b), it appears that PGIR 20ekz and PGIR 20eig do not meet this requirement, and they could have been discovered retroactively by other means. As seen in Figure 8 from De et al. (2021b), if the sample of PGIR novae was decreased from 11 to 9 novae (by excluding 20ekz and 20eig), it would correspond to a 1σ range for the Galactic nova rate between 27 and 52 yr^{-1}, consistent with both the PGIR rate and the rate derived in this work. Hence, the rates derived in this work are inconsistent at the 1σ level with the PGIR rate, but small changes in either model would appear to bring the results into agreement at a rate of $\sim$30 yr^{-1}.

5.3. Extragalactic Comparisons and Faint/Fast Novae

Because of uncertainties in galaxy stellar masses and the potential variation of nova rate with stellar population parameters, there are challenges associated with comparing indirectly derived rates from extragalactic nova surveys with direct rates from Galactic surveys. However, extragalactic surveys have historically been more complete in at least some dimensions, so the exercise has been common practice in the literature. As seen in Figure 1, extragalactic studies typically lead to lower Galactic rate estimates than direct measurements. The microlensing survey of M31 suggested a Milky Way rate of $R = 34^{+15}_{-12}$ yr^{-1} (Darnley et al. 2006), consistent with the rates derived here. Additionally, the 20 yr survey of M31 recently indirectly derived a Galactic nova rate of $R = 28^{+5}_{-4}$ yr^{-1} (Rector et al. 2022), also consistent with our rate at the 1σ level. Another common practice is to estimate the linear correlation between the nova rate and the log luminosity of a sample of galaxies. Della Valle & Livio (1994b) studied five galaxies to infer a Galactic nova rate of 24 yr^{-1}, Shafter et al. (2000) studied three galaxies to infer a Galactic nova rate of 27^{+10}_{-8} yr^{-1}, Shafter et al. (2014) gathered measurements from 16 galaxies to arrive at a Galactic rate of $\sim$25 yr^{-1}, and Della Valle & Izzo (2020) compiled measurements from 14 galaxies to infer a Galactic nova rate of $\sim$22 yr^{-1}. These estimates have large and unreported uncertainties, but they are notably all consistent at the 1σ level with the most likely rate predicted in this work.

Shara et al. (2016) argue that extragalactic nova surveys underestimate nova rates because they neglect to account for faint and fast novae, but the present paper shows that missed faint, fast novae are not an important source of uncertainty in the Galactic nova rate (see Section 3.2 and Figure 5) compared to other factors such as the foreground extinction. This conclusion is consistent with the lack of discovery of a substantial population of faint, fast novae after years of daily monitoring by ASAS-SN. While faint, fast novae undoubtedly exist at some level and are harder to detect, current Galactic data provide no evidence for a large yet-to-be-discovered population of these sources, and it is plausible that extragalactic studies have overestimated their importance.

6. Conclusions

In this work, we have presented the results of the first direct Galactic nova rate analysis using optical all-sky transient surveys. The results predict a lower rate than recent estimates, with the most likely model, built by combining ASAS-SN and Gaia observations, estimating a Galactic nova rate of $R = 26 \pm 5$ yr^{-1}. This rate is consistent with the derived rates from ASAS-SN and Gaia observations individually. Our analysis suggests that rates above 40 yr^{-1} are unlikely unless (i) novae have a much lower scale height than predicted from stellar density models (subjecting them to higher dust extinction), (ii) the typical extinction is much higher than predicted from existing three-dimensional dust models, or (iii) the reporting efficiencies of ASAS-SN and Gaia are much lower than indicated from current evidence.

If the Galactic nova rate is < 30 yr^{-1}, does that have any broader implications for the Galaxy? Izzo et al. (2015) detected ^{7}Li absorption in V1369 Cen and suggested that, based on the intensity of the line, novae could explain the overabundance of ^{7}Li by assuming a slow nova rate of 24 yr^{-1}. On the other hand, Molaro et al. (2016) argue that only two novae per year would be necessary to explain the abundance of ^{7}Li in the Galaxy. Hence, it is possible that even a relatively low nova rate could still explain the Galactic abundances of ^{7}Li.

Our derived rate suggests that, over the past 5 yr, observers have been discovering about half of the Galaxy's nova eruptions. Between 2019 and 2021, we find that ASAS-SN and Gaia observations alone have recovered $\sim$54% of Galactic novae, and individually, ASAS-SN recovers $\sim$33% of novae and Gaia recovers $\sim$42% of novae. This implies that the recovery efficiency of Galactic novae by amateur astronomers over the past few decades has been much higher than previously suggested.

Though direct estimates of the Galactic nova rate from large time-domain surveys allow for fewer assumptions regarding cadence, many assumptions about the pipelines still need to be made. This is likely the reason the rates derived in this work do not agree with the PGIR rate, but we find that small changes in the models can increase the agreement, with the largest overlap occurring at $\sim$30 novae per year.

While it is important to improve our understanding of the efficiency of transient alert pipelines (perhaps though uninformed "injection" events, as performed by LIGO/Virgo; Abadie et al. 2012), we can also make progress by gathering additional data from surveys with improved cadences and less sensitivity to dust. As seen in Figure 8, the number of northern

hemisphere Galactic plane novae discovered exceeded that in the southern plane. Given that there are currently more operating surveys covering the northern plane than the southern plane, and that some northern surveys are less sensitive to dust (such as PGIR), a red or near-IR high-resolution and moderate-cadence survey of the southern Galactic plane would give close to all-sky coverage of the dusty regions of the Galaxy, allowing the role of dust in nova discovery to be better constrained. Luckily, planned near-IR surveys like the Dynamic REd All-sky Monitoring Survey (DREAMS; Soon et al. 2020) and the PRime-focus Infrared Microlensing Experiment[17] (PRIME), along with the multiband optical Vera Rubin Observatory (Tyson 2002), make the future prospects of southern hemisphere time-domain surveys bright. Depending on the observing strategy to cover the plane, these surveys should have the ability to detect novae not recovered by current observing capabilities. The degree to which these surveys increase the discovery rate will be the next big step in constraining the Galactic nova rate. With additional southern hemisphere observations, the transient community could discover up to ∼80% of the Galactic nova population, leading to a tightly constrained Galactic nova rate.

A.K., L.C., E.A., and K.V.S. acknowledge financial support of NSF award AST-1751874 and a Cottrell fellowship of the Research Corporation. J.S. acknowledges support from the Packard Foundation. B.J.S., C.S.K., and K.Z.S. are supported by NSF grant AST-1907570. C.S.K. and K.Z.S. are supported by NSF grant AST-181440. S.T.H. is funded by the Science and Technology Facilities Council grant ST/S000623/1. Z.K.-R. acknowledges funding from the Netherlands Research School for Astronomy (NOVA).

We thank the Las Cumbres Observatory and its staff for its continuing support of the ASAS-SN project. ASAS-SN is supported by the Gordon and Betty Moore Foundation through grant GBMF5490 to the Ohio State University and NSF grants AST-1515927 and AST-1908570. Development of ASAS-SN has been supported by NSF grant AST-0908816, the Mt. Cuba Astronomical Foundation, the Center for Cosmology and AstroParticle Physics at the Ohio State University, the Chinese Academy of Sciences South America Center for Astronomy (CAS- SACA), and the Villum Foundation.

This work has made use of data from the European Space Agency (ESA) mission Gaia (https://www.cosmos.esa.int/gaia), processed by the Gaia Data Processing and Analysis Consortium (DPAC, https://www.cosmos.esa.int/web/gaia/dpac/consortium). Funding for the DPAC has been provided by national institutions, in particular the institutions participating in the Gaia Multilateral Agreement. Further details of funding authorities and individuals contributing to the success of the mission is shown at https://gea.esac.esa.int/archive/documentation/GEDR3/Miscellaneous/sec_acknowl/.

This work is in part based on observations obtained at the Southern Astrophysical Research (SOAR) telescope, which is a joint project of the Ministério da Ciência, Tecnologia e Inovações (MCTI/LNA) do Brasil, the US National Science Foundations NOIRLab, the University of North Carolina at Chapel Hill (UNC), and Michigan State University (MSU).

The analysis for this work was performed primarily in `ipython` (Perez & Granger 2007) using `numpy` (Oliphant 2006; Van Der Walt et al. 2011), `Astropy` (Astropy Collaboration et al. 2018), `Matplotlib` (Hunter 2007), and `scipy` (Virtanen et al. 2020).

We thank K. De for helpful conversations regarding Galactic novae and transient surveys and J. Bovy for help with the extinction models. We also thank the anonymous referee for insightful comments.

[17] http://www-ir.ess.sci.osaka-u.ac.jp/prime/index.html

ORCID iDs

A. Kawash https://orcid.org/0000-0003-0071-1622
L. Chomiuk https://orcid.org/0000-0002-8400-3705
J. Strader https://orcid.org/0000-0002-1468-9668
K. V. Sokolovsky https://orcid.org/0000-0001-5991-6863
E. Aydi https://orcid.org/0000-0001-8525-3442
C. S. Kochanek https://orcid.org/0000-0001-6017-2961
K. Mukai https://orcid.org/0000-0002-8286-8094
B. Shappee https://orcid.org/0000-0003-4631-1149
T. Jayasinghe https://orcid.org/0000-0002-6244-477X
T. W.-S. Holoien https://orcid.org/0000-0001-9206-3460
J. L. Prieto https://orcid.org/0000-0003-0943-0026

References

Abadie, J., Abbott, B. P., Abbott, R., et al. 2012, PhRvD, 85, 082002
Allen, C. W. 1954, MNRAS, 114, 387
Arnould, M., & Norgaard, H. 1975, A&A, 42, 55
Astropy Collaboration, Price-Whelan, A. M., Sipőcz, B. M., et al. 2018, AJ, 156, 123
Aydi, E., Buckley, D. A. H., Chomiuk, L., et al. 2019a, ATel, 13134, 1
Aydi, E., Buckley, D. A. H., Chomiuk, L., et al. 2019b, ATel, 12795, 1
Aydi, E., Buckley, D. A. H., Chomiuk, L., et al. 2020a, ATel, 13867, 1
Aydi, E., Buckley, D. A. H., Chomiuk, L., et al. 2020b, ATel, 13872, 1
Aydi, E., Sokolovsky, K. V., Kawash, A., Strader, J., & Chomiuk, L. 2021, ATel, 14880, 1
Aydi, E., Sokolovsky, K. V., Strader, J., Chomiuk, L., & Kawash, A. 2020c, ATel, 13449, 1
Aydi, E., Strader, J., Chomiuk, L., et al. 2019c, ATel, 13027, 1
Aydi, E., Strader, J., Chomiuk, L., et al. 2019d, ATel, 13068, 1
Aydi, E., Strader, J., Chomiuk, L., et al. 2020d, ATel, 13517, 1
Bennett, M. B., Wrede, C., Chipps, K. A., et al. 2013, PhRvL, 111, 232503
Bovy, J., Rix, H.-W., Green, G. M., Schlafly, E. F., & Finkbeiner, D. P. 2016, ApJ, 818, 130
Capaccioli, M., Della Valle, M., D'Onofrio, M., & Rosino, L. 1989, AJ, 97, 1622
Cautun, M., Benítez-Llambay, A., Deason, A. J., et al. 2020, MNRAS, 494, 4291
Chambers, K. C., Magnier, E. A., Metcalfe, N., et al. 2016, arXiv:1612.05560
Chen, H.-L., Woods, T. E., Yungelson, L. R., Gilfanov, M., & Han, Z. 2016, MNRAS, 458, 2916
Chomiuk, L., Metzger, B. D., & Shen, K. J. 2021, ARA&A, 59, 391
Ciardullo, R., Ford, H. C., Williams, R. E., Tamblyn, P., & Jacoby, G. H. 1990, AJ, 99, 1079
Clemens, J. C., Crain, J. A., & Anderson, R. 2004, Proc. SPIE, 5492, 331
Darnley, M. J., Bode, M. F., Kerins, E., et al. 2006, MNRAS, 369, 257
Darnley, M. J., Henze, M., Steele, I. A., et al. 2015, A&A, 580, A45
De, K., Hankins, M., Andreoni, I., et al. 2020a, ATel, 14014, 1
De, K., Hankins, M., Kasliwal, M. M., et al. 2019, ATel, 13130, 1
De, K., Hankins, M., Kasliwal, M. M., et al. 2020b, ATel, 13790, 1
De, K., Hankins, M., Kasliwal, M. M., et al. 2020c, ATel, 13817, 1
De, K., Hankins, M., Kasliwal, M. M., et al. 2020d, ATel, 13914, 1
De, K., Hankins, M. J., Kasliwal, M. M., et al. 2020f, PASP, 132, 025001
De, K., Hankins, M., Kasliwal, M. M., et al. 2020e, ATel, 14062, 1
De, K., Hankins, M., Hillenbrand, L., et al. 2021a, ATel, 14950, 1
De, K., Kasliwal, M. M., Hankins, M. J., et al. 2021b, ApJ, 912, 19
De, K., Kawash, A., Kasliwal, M. M., et al. 2021c, ATel, 14677, 1
De, K., Perley, D., Andreoni, I., et al. 2021d, ATel, 14657, 1
Della Valle, M., & Izzo, L. 2020, A&ARv, 28, 3
della Valle, M., & Livio, M. 1994a, A&A, 286, 786
della Valle, M., & Livio, M. 1994b, ApJL, 423, L31
della Valle, M., & Livio, M. 1995, ApJ, 452, 704
Diehl, R., Halloin, H., Kretschmer, K., et al. 2006, Natur, 439, 45

Dilday, B., Howell, D. A., Cenko, S. B., et al. 2012, Sci, 337, 942
Drimmel, R., Cabrera-Lavers, A., & López-Corredoira, M. 2003, A&A, 409, 205
Duerbeck, H. W. 2008, in Classical Novae (Cambridge Astrophysics Series, No. 43) ed. M. F. Bode & A. Evans (2nd Edition; Cambridge: Cambridge Univ. Press), 1
Gaia Collaboration, Brown, A. G. A., Vallenari, A., et al. 2021, A&A, 649, A1
Gaia Collaboration, Prusti, T., de Bruijne, J. H. J., et al. 2016, A&A, 595, A1
Gaia Collaboration, Spoto, F., Tanga, P., et al. 2018, A&A, 616, A13
Geary, K., & Amorim, A. 2021, CBET, 5013, 1
Green, G. M., Schlafly, E., Zucker, C., Speagle, J. S., & Finkbeiner, D. 2019, ApJ, 887, 93
Hatano, K., Branch, D., Fisher, A., & Starrfield, S. 1997, MNRAS, 290, 113
Hodgkin, S. T., Delgado, A., Harrison, D. L., et al. 2021a, ATel, 14402, 1
Hodgkin, S. T., Harrison, D. L., Breedt, E., et al. 2021b, A&A, 652, A76
Hunter, J. D. 2007, CSE, 9, 90
Izzo, L., Della Valle, M., Mason, E., et al. 2015, ApJL, 808, L14
Jayasinghe, T., Kochanek, C. S., Stanek, K. Z., et al. 2018, MNRAS, 477, 3145
José, J., & Hernanz, M. 1998, ApJ, 494, 680
Joshi, V., Borthakur, S., Banerjee, D. P. K., & Srivastava, M. K. 2021, ATel, 14544, 1
Kalomeni, B., Nelson, L., Rappaport, S., et al. 2016, ApJ, 833, 83
Karambelkar, V., De, K., Hall, X., & Kasliwal, M. M. 2021, ATel, 14744, 1
Kasliwal, M. M., Cenko, S. B., Kulkarni, S. R., et al. 2011, ApJ, 735, 94
Kawash, A., Aydi, E., Strader, J., Chomiuk, L., & Sokolovsky, K. V. 2020, ATel, 14118, 1
Kawash, A., Aydi, E., Strader, J., Sokolovsky, K. V., & Chomiuk, L. 2021a, ATel, 14928, 1
Kawash, A., Aydi, E., Strader, J., Sokolovsky, K. V., & Chomiuk, L. 2021b, ATel, 14957, 1
Kawash, A., Aydi, E., Velez, P., et al. 2021c, ATel, 15001, 1
Kawash, A., Chomiuk, L., Rodriguez, J. A., et al. 2021d, ApJ, 922, 25
Kawash, A., Chomiuk, L., Strader, J., et al. 2021e, ApJ, 910, 120
Kemp, A. J., Karakas, A. I., Casey, A. R., et al. 2021, MNRAS, 504, 6117
Kochanek, C. S., Shappee, B. J., Stanek, K. Z., et al. 2017, PASP, 129, 104502
Kojima, T., & Nishimura, H. 2020, CBET, 4848, 1
Kopylov, I. M. 1955, Izvestiya Krymskoj Astrofizicheskoj Observatorii, 13, 23
Kostrzewa-Rutkowska, Z., Jonker, P. G., Hodgkin, S. T., et al. 2018, MNRAS, 481, 307
Li, L., Shen, S., Hou, J., et al. 2018, ApJ, 858, 75
Liller, W., & Mayer, B. 1987, PASP, 99, 606
Lundmark, K. 1935, MeLuS, 74, 1
Maehara, H., Taguchi, K., Tampo, Y., Kojiguchi, N., & Isogai, K. 2021, ATel, 14471, 1
Marshall, D. J., Robin, A. C., Reylé, C., Schultheis, M., & Picaud, S. 2006, A&A, 453, 635
Metzger, B. D., Zenati, Y., Chomiuk, L., Shen, K. J., & Strader, J. 2021, ApJ, 923, 100
Molaro, P., Izzo, L., Mason, E., Bonifacio, P., & Della Valle, M. 2016, MNRAS, 463, L117
Mróz, P., Udalski, A., Poleski, R., et al. 2015, ApJS, 219, 26
Munari, U., Castellani, F., Dallaporta, S., & Andreoli, V. 2020, ATel, 14224, 1
Munari, U., Vagnozzi, A., & Valisa, P. 2021a, ATel, 14793, 1
Munari, U., Valisa, P., & Dallaporta, S. 2021b, ATel, 14704, 1
Nataf, D. M., Gonzalez, O. A., Casagrande, L., et al. 2016, MNRAS, 456, 2692
Nelemans, G., Siess, L., Repetto, S., Toonen, S., & Phinney, E. S. 2016, ApJ, 817, 69
Oliphant, T. E. 2006, A Guide to NumPy, 1 (USA: Trelgol Publishing)
Özdönmez, A., Ege, E., Güver, T., & Ak, T. 2018, MNRAS, 476, 4162
Pala, A. F., Gänsicke, B. T., Belloni, D., et al. 2022, MNRAS, 510, 6110
Patat, F., Chugai, N. N., Podsiadlowski, P., et al. 2011, A&A, 530, A63
Patterson, J., Uthas, H., Kemp, J., et al. 2013, MNRAS, 434, 1902
Perez, F., & Granger, B. E. 2007, CSE, 9, 21
Pickering, E. C. 1893, AN, 134, 101
Pickering, W. H. 1895, Obs, 18, 436
Pojmański, G. 2001, in ASP Conf. Ser., IAU Colloq. 183: Small Telescope Astronomy on Global Scales, 246, ed. B. Paczynski, W.-P. Chen, & C. Lemme (San Francisco, CA: ASP), 53
Prantzos, N. 2012, A&A, 542, A67
Rector, T. A., Shafter, A. W., Burris, W. A., et al. 2022, ApJ, 936, 117
Robin, A. C., Reylé, C., Derrière, S., & Picaud, S. 2003, A&A, 409, 523
Romano, D., Matteucci, F., Ventura, P., & D'Antona, F. 2001, A&A, 374, 646
Rukeya, R., Lü, G., Wang, Z., & Zhu, C. 2017, PASP, 129, 074201
Schaefer, B. E. 2018, MNRAS, 481, 3033
Schenker, K., Kolb, U., & Ritter, H. 1998, MNRAS, 297, 633
Schreiber, M. R., Zorotovic, M., & Wijnen, T. P. G. 2016, MNRAS, 455, L16
Shafter, A. W. 1997, ApJ, 487, 226
Shafter, A. W. 2002, in AIP Conf. Ser., 637, Classical Nova Explosions, ed. M. Hernanz & J. José (Melville, NY: AIP), 462
Shafter, A. W. 2017, ApJ, 834, 196
Shafter, A. W., Ciardullo, R., & Pritchet, C. J. 2000, ApJ, 530, 193
Shafter, A. W., Curtin, C., Pritchet, C. J., Bode, M. F., & Darnley, M. J. 2014, in ASP Conf. Ser., 490, Stellar Novae: Past and Future Decades, ed. P. A. Woudt & V. A. R. M. Ribeiro (San Francisco, CA: ASP), 77
Shafter, A. W., Darnley, M. J., Hornoch, K., et al. 2011, ApJ, 734, 12
Shafter, A. W., & Irby, B. K. 2001, ApJ, 563, 749
Shafter, A. W., Rau, A., Quimby, R. M., et al. 2009, ApJ, 690, 1148
Shappee, B. J., Prieto, J. L., Grupe, D., et al. 2014, ApJ, 788, 48
Shara, M. M., Doyle, T. F., Lauer, T. R., et al. 2016, ApJS, 227, 1
Shara, M. M., Doyle, T., Lauer, T. R., et al. 2017a, ApJ, 839, 109
Shara, M. M., Iłkiewicz, K., Mikołajewska, J., et al. 2017b, Natur, 548, 558
Sharov, A. S. 1972, SvA, 16, 41
Simion, I. T., Belokurov, V., Irwin, M., et al. 2017, MNRAS, 471, 4323
Sokolovsky, K., Aydi, E., Chomiuk, L., et al. 2020, ATel, 13903, 1
Sokolovsky, K., Korotkiy, S., & Lebedev, A. 2014, in ASP Conf. Ser., Stellar Novae: Past and Future Decades, 490, ed. P. A. Woudt & V. A. R. M. Ribeiro (San Francisco, CA: ASP), 395
Soon, J., Adams, D., De, K., et al. 2020, Proc. SPIE, 11203, 1120307
Soria, R., De, K., Kasliwal, M. M., et al. 2021, ATel, 14567, 1
Sparks, W. M., & Sion, E. M. 2021, ApJ, 914, 5
Srivastava, M. K., Kumar, V., Banerjee, D. P. K., & Joshi, V. 2021, ATel, 14487, 1
Starrfield, S., Bose, M., Iliadis, C., et al. 2020, ApJ, 895, 70
Starrfield, S., Truran, J. W., & Sparks, W. M. 1978, ApJ, 226, 186
Strader, J., Chomiuk, L., Aydi, E., et al. 2019a, ATel, 13047, 1
Strader, J., Chomiuk, L., Swihart, S., et al. 2019b, ATel, 13112, 1
Strope, R. J., Schaefer, B. E., & Henden, A. A. 2010, AJ, 140, 34
Taguchi, K., Kawabata, M., Yamanaka, M., & Isogai, K. 2021, ATel, 14513, 1
Tajitsu, A., Sadakane, K., Naito, H., Arai, A., & Aoki, W. 2015, Natur, 518, 381
Toonen, S., Claeys, J. S. W., Mennekens, N., & Ruiter, A. J. 2014, A&A, 562, A14
Tyson, J. A. 2002, Proc. SPIE, 4836, 10
Udalski, A., Szymański, M. K., & Szymański, G. 2015, AcA, 65, 1
van den Bergh, S. 1991a, PASP, 103, 609
van den Bergh, S. 1991b, PASP, 103, 1053
van den Bergh, S., & Younger, P. F. 1987, A&AS, 70, 125
Van Der Walt, S., Colbert, S. C., & Varoquaux, G. 2011, CSE, 13, 22
Vasini, A., Matteucci, F., & Spitoni, E. 2022, arXiv:2204.00510
Virtanen, P., Gommers, R., Oliphant, T. E., et al. 2020, NatMe, 17, 261
Walter, F. M., Battisti, A., Towers, S. E., Bond, H. E., & Stringfellow, G. S. 2012, PASP, 124, 1057
Warner, B. 2008, in Properties of novae: An overview, ed. M. F. Bode & A. Evans (Cambridge: Cambridge Univ. Press), 16
Williams, S. C., Darnley, M. J., Healy, M. W., Murphy-Glaysher, F. J., & Ransome, C. L. 2019, ATel, 13241, 1